NANOENGINEERED SURFACES AND CARBON NANOTUBE CONJUGATED MICROWIRE BIOSENSOR FOR MICROBIAL CONTROL AND DETECTION

A THESIS SUBMITTED TO THE GRADUATE DIVISION OF THE UNIVERSITY OF HAWAIʻI AT MĀNOA IN PARTIAL FULFILLMENT OF THE REQUIREMENTS FOR THE DEGREE OF

MASTER OF SCIENCE

IN

FOOD SCIENCE

DECEMBER 2019

By

Bog Eum Lee

Thesis Committee:

Soojin Jun, Chairperson

Yong Li

Kacie Ho

ACKNOWLEDGEMENTS

I would like to express my deepest appreaction to my advisor, Dr. Soojin Jun, for all his support and guidance throughout my education. He gaved me the opportunity to be a part of the Food Processing lab when I just started the food science master's program. I had countless valuable experiences and with his help, I have grown both academically and as a person. As I start a new chapter in my life, I will engrain the lessons I have learned and remember this life-changing adventure.

I would like to thank Dr. Yong Li, for the warm encouragement, constructive comments, and kindly allowing me to work in the Food Microbiology Lab. The knowledge about food microbiology from his teachings have had substantial influence on my research and have engaged me into the food microbiology world. I would also like to thank Dr. Kacie Ho, for her insightful teachings, heartfelt word of suggestions, and kindly offering her help at all times.

I would like to convey my sincere gratitude for my previous and current labmates. They have always been supportive and offered advice in difficult moments. Especially Inae Lee, who trained me lab techniques when I was just starting my experiments, as well as Cherisse, Raymond, TY, Sean, Yu, Dr. Youngsang You and his family, for their kindness and help. I will always be grateful and remember our fun time spent together in the Food Processing Lab.

Finally, I would like to thank my family members and friends for their patience and encouragement given to me at all times. Especially my parents and grandparents, who have showered me with blessings and love. This completion would not have been possible without their prayers and I thank them with all my heart.

ABSTRACT

Nanotechnology is applied in various fields including the food industry. Nanotechnology integrates several disciplines and uses nanomaterials with size in the range from 1 to 100 nm. In the food industry, nanotechnology has potential to cover many aspects such as product development, food security, and new functional materials. Particularly, nanotechnology is a promising tool to address public food safety concerns by reducing the consumption of contaminated food products.

Over the past years, the demand for real-time and sensitive detection of pathogenic bacteria in food has increased significantly. Current detection methods cannot facilitate the needs of food processors due to limitations such as time, cost, and mandatory laboratory settings. Therefore, a biosensor-based detection technology, which has advantages such as high sensitivity and portability, has emerged as an alternative. With the rapid advancement of nanotechnology, various nanomaterials have been integrated into biosensing platforms to address challenges such as sensitivity and rapid response time.

In this study, a single-walled carbon nanotube (SWCNT)-based electrochemical impedance immunosensor for on-site detection of *Listeria monocytogenes (L. monocytogenes)* was developed. The *L. monocytogenes* immunosensor was functionalized by coating a gold plated tungsten wire with polyethylenimine, SWCNTs, streptavidin, biotinylated *L. monocytogenes* antibodies, and bovine serum albumin to induce specificity and selectivity. A linear relationship (R^2 = 0.982) was observed between the electron transfer resistance measurements and concentrations of *L. monocytogenes* in the range of 10^3 - 10^8 CFU/mL. In addition, the sensor detected *L. monocytogenes* without significant interference in the presence of other bacterial cells

such as *Salmonella* Typhimurium and *Escherichia coli* O157:H7. To address the needs of on-site monitoring, the sensor was integrated into a smartphone-controlled biosensor platform. The performance of the smartphone-controlled platform was evaluated with a conventional laboratory instrument. The sensing signals of the sensors immune-reacted with 10^3 - 10^5 CFU/mL of *L. monocytogenes* measured with both devices were not significantly different. The feasibility of the proposed platform for use in real food samples was examined with a lettuce homogenate. The recovery of the lettuce homogenates spiked with 10^3 - 10^5 CFU/mL of *L. monocytogenes* ranged from 90.21% to 93.69%, which proved to be suitable for food samples. Therefore, the developed on-site applicable SWCNT-based immunosensor platform appeared to be a promising tool to be used in field settings for food and agricultural applications.

In order to additionally reduce the risk of microbial food contamination, nanotechnology has been extensively utilized to control biofilm formation. Bacterial adhesion on food-contact surfaces results in biofilm formation and imposes a significant challenge to food safety. Current biofilm control strategy is operating routine cleaning using chemical disinfectants. The main limitation of this method is its efficacy is altered by organic materials, pH, and temperature. It has been recognized that surface engineering could mitigate the level of bio-contamination by controlling the topography and physicochemistry of the substrate. As a result, superhydrophobic (SH) surface, which is known to be self-cleanable, has emerged as an alternative. SH surface has a water contact angle (WCA) greater than 150° and can be produced by introducing low surface energy nanoscale roughness on food-contact surface. Although there are many methods to produce SH surface, a combination of electrochemical etching and polytetrafluoroethylene (PTFE) coating has been suggested as an efficient technique due to the possibility of controlling surface morphologies and ease of operation.

In this study, surface alterations on stainless steel were performed with electrochemical etching and PTFE film. The substrate was electrochemically etched at various conditions to induce nanoscale roughness and coated with PTFE to lower the surface energy. The nanostructures produced on the stainless steel substrates were characterized by field emission scanning electron microscopy. The stainless steel substrates etched at 10 V for 5 min and 10 V for 10 min with PTFE deposition resulted in an average WCA of 154° ± 4° with pore diameter of 50 nm. The bacterial resistance of these substrates (154° ± 4°) was evaluated by adhering 60 µL of *L. monocytogenes* (10^8 CFU/mL) on the substrates for 24 hours. As compared to the bare substrate, these SH surfaces significantly inhibited the bacterial adhesion up to 99%. The anti-biofilm characteristic of the superhydrophobic substrate (10 V 5 min with PTFE) was further evaluated with a CDC biofilm reactor and the bacteria entrapped in the biofilms were reduced by 98.4%. This nanoscale surface modification technique showed the feasibility for use as anti-microbial and anti-biofilm surfaces in the food industry.

Table of Contents

LIST OF FIGURES

LIST OF TABLES

LIST OF ABBREVIATIONS

AC	Alternating current
AgNP	Silver nanoparticle
ANOVA	Analysis of variance
Au	Gold
AuNF	Gold nanoflower
AuNP	Gold nanoparticle
BSA	Bovie serum albumin
CDC	U.S. Center for Disease Control and Prevention
Cdl	Double-layer capacitance
CdTe	Cadmium telluride
C-F	Carbon-fluorine
CFU	Colony forming unit
Cl^-	Chloride
CPU	Central processing unit
DC	Direct current
DMF	N, N-dimethylformamide
DNA	Deoxyribonucleic acid
EIS	Electrochemical impedance spectroscopy
ELISA	Enzyme-linked immunosorbent assay
EPS	Extracellular polymeric substances
f	frequency
f_1	Air fraction
f_2	Surface fraction
Fe	Iron
Fe^{2+}	Ferrous ions
FESEM	Field emission scanning electron microscope
FET	Field effect transistor
H^+	Hydrogen ion
HCl	Hydrochloric acid
HDMS	Hexamethyldisilazane
HNO_3	Nitric acid
I_0	Maximum current
IMB	Immunomagnetic bead
LOD	Limit of detection
MWCNT	Multi-walled carbon nanotube
mN	Millinewton
NO_3^-	Nitrate
PBS	Phosphate buffered saline
PCR	Polymerase chain reaction
PDMS	Polydimethylsiloxane
PEI	Polyethylenimine
ppm	Parts per million

PTFE	Polytetrafluoroethylene
Ret	Electron transfer resistance
RNA	Ribonucleic acid
r_s	Roughness factor
Rs	Electrolyte solution resistance
S	Siemens
SERS	Surface-enhanced Raman spectroscopy
SH	Superhydrophobic
SPR	Surface plasmon resonance
SWCNT	Single-walled carbon nanotube
t	Time
TiO_2	Titanium dioxide
TSB	Tryptic soy broth
V	Applied voltage
V_0	Maximum voltage
V_S	Speed of etching along the surface
V_T	Speed of etching along the track
WCA	Water contact angle
WHO	World Health Organization
Y	Complex conductance
Z'	Real impedance
Z''	Imaginary conductance
Zw	Warburg impedance
ΔRet	Change in electron transfer resistance
φ	Phase shift
γ_{LV}	Liquid surface tension
γ_{SL}	Solid-liquid interfacial energy
γ_{SV}	Solid surface energy
θ_c	Cassie-Baxter apparent contact angle
θ_W	Wenzel apparent contact angle
θ_Y	Young's contact angle

Chapter 1.

INTRODUCTION

Nanotechnology refers to the use of nanomaterials at dimensions of roughly 1 to 100 nanometers. Nanomaterials exhibit different dimensions based on their structural elements such as zero dimension (quantum dots, or nanoclusters), one-dimension (nanorods or nanotubes), two-dimension (thin films), and three-dimensions (nanocomposites) in the nano-size range (Pathakoti, Manubolu & Hwang, 2017; Bajpai et al., 2018). These nanomaterials adopt unique properties which are attractive for various applications and are already in-use in diverse fields such as computer electronics, energy production, and medicine (Bajpai et al., 2018; Sozer & Kokini, 2009). Although relatively recent, it has been shown that nanotechnology has a significant potential to advance current food systems and processing. The possible applications of nanotechnology in the food industry are illustrated in Figure 1.1. One of the major links of nanotechnology to the food sector is food safety. Food is a universal human need and thus, securing food safety is critical. Despite the improved food safety management practices and hygiene control systems, the number of foodborne illness outbreaks has increased due to consumers' demands for minimally processed foods and globalization of the food supply (Kruse, 1999; Patrignani et al., 2015). As a result, numerous nanomaterials have been synthesized to enhance food safety in terms of screening food products for the presence of pathogens and inhibiting bacterial adhesion on food-contact surfaces (Bajpai et al., 2018).

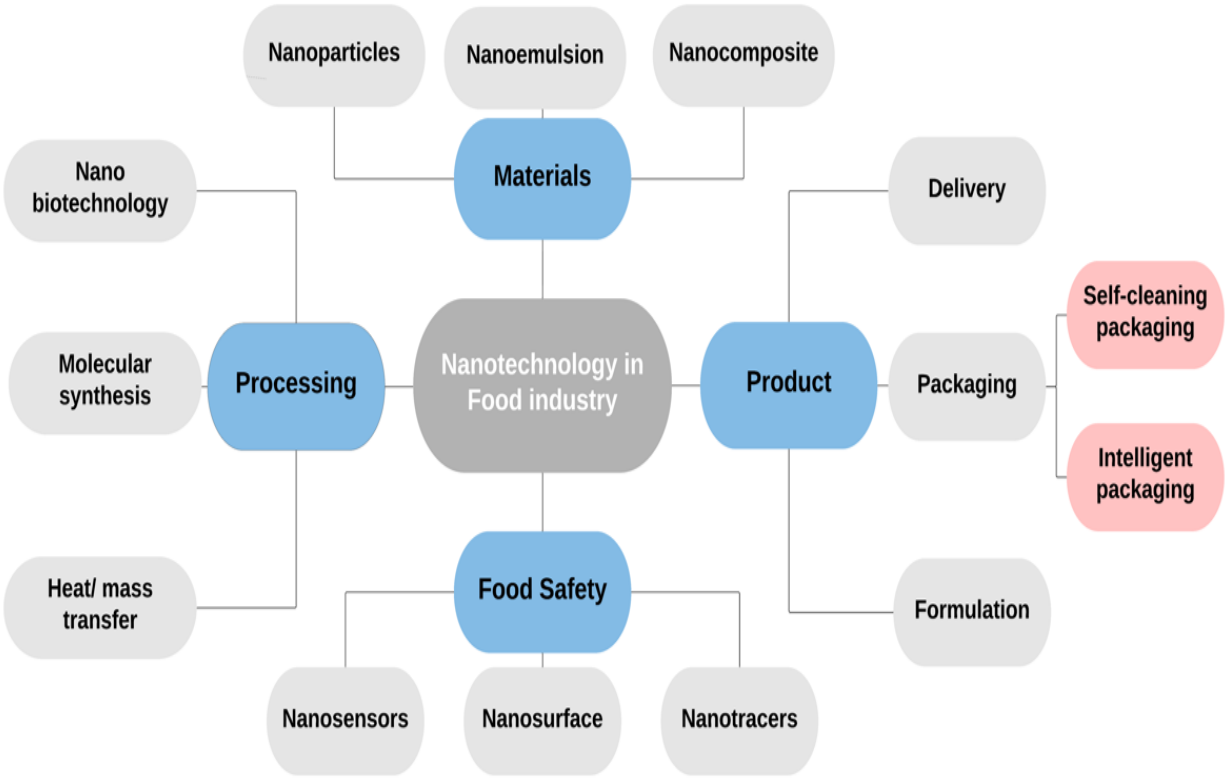

Figure 1.1. Applications of nanotechnology in the food industry (Modified from Berekaa, 2015).

Up to date, the conventional detection methods such as microscopy and cell culture, biochemical assays, and immunological tests have been in use for food safety screening (Velusamy et al., 2010). Although sensitive, in terms of the sensing rapidity, these methods are time-consuming and inadequate to meet the needs of food processors and regulatory agencies (Alocilja & Radke, 2003). Therefore, biosensor technology has emerged as an alternative. A biosensor is an analytical device which converts a specific biological event into a measurable signal. The biosensor is composed of a bioreceptor, which couples with the target analyte, and a transducer to convert the recognition event into a detectable signal (Ahmed et al., 2014; Singh, Poshtiban & Evoy, 2013). Amongst many functional nanomaterials, a single-walled carbon nanotube (SWCNT) is regarded as the most attractive nanomaterial to construct biosensor platforms due to their unique structural, mechanical, and electrical properties. The large surface area of SWCNT increases the

number of immobilized bioreceptors on the sensors and their sensitive responses to changes in the surrounding environment are known to enhance the sensing performance (Sireesha et al., 2018).

In addition to food screening techniques, it is important to impart bacterial resistance on food-contact surfaces (Costa, Luciano & Pasa, 2013). In the food processing environment, the adherence of pathogens on food-contact surfaces is often observed and thus, result in the formation of biofilms. The biofilms cause detrimental effects such as cross-contamination, transmission of diseases, as well as inefficient heat transfer (Garrett, Bhakoo & Zhang, 2008; Sandu & Singh, 1991). Bacterial attachment is a complex process and thus, surface engineering has emerged to reduce bacterial adhesion (Simões, Simões & Vieira, 2010). Amongst the many surface modifications, superhydrophobic surfaces (water contact angle > 150°) have gained a significant interest due to their extremely non-wettable properties and the low adhesion force between the bacteria and the surface. This unique surface can be fabricated by lowering the surface energy and introducing nanoscale roughness with the aid of nanotechnology (Gu & Ren, 2014; Zhang, Wang & Levänen, 2013). Electrochemical etching is a technique which can produce various surface morphologies including nanoscale patterns by removing metals. This method is known to be relatively fast and easy to use. Therefore, electrochemical etching in combination with PTFE coating is expected to produce a superhydrophobic substrate by introducing nanoscale pores with low surface energy.

The goal of this research was to explore the effects of SWCNTs in an electrochemical impedance immunosensor for the detection of foodborne pathogen and evaluate the sensitivity, specificity, and selectivity of the biosensor. In addition, the developed biosensor was incorporated into a smartphone-based unit for on-site detection of *L. monocytogenes* in peptone water and a food sample. In addition, a nanoengineered food-contact surface was developed to overcome

bacterial attachment and thus, biofilm formation by utilizing electrochemical etching and PTFE coatings. Specific objectives leading to these goals were:

Objective 1: Evaluate a SWCNT-conjugated electrochemical impedance immunosensor for the detection of *L. monocytogenes* in both pure and bacterial mixtures

Objective 2: Develop an on-site applicable a SWCNT-conjugated biosensor with a smartphone-controlled unit for the detection of a single analyte in peptone water and lettuce homogenate

Objective 3: Develop a protocol to produc a superhydrophobic stainless steel substrate via electrochemical etching with PTFE coating

Objective 4: Evaluate bacterial and biofilm resistance of the fabricated superhydrophobic surface

Chapter 2.

LITERATURE REVIEW

2.1. Introduction

This chapter includes the impact of foodborne pathogens, conventional detection methods, as well as nanomaterial-based biosensors for food safety monitoring. In addition, the significance of biofouling and the development of anti-biofouling surfaces using nanotechnology will also be discussed.

2.1.1. Foodborne pathogens and illness outbreaks

Despite many interventions and prevention efforts, food safety remains as a persistent problem in the world. According to the World Health Organization (WHO), foodborne illnesses are diseases caused by agents that enter the body through the ingestion of food (Velusamy et al., 2010). In 2019, the WHO reported that in Europe, more than 23 million people are sickened from consumption of contaminated foods and 4,700 die per year. The Centers for Disease Control and Prevention (CDC) estimates each year, 1 in 6 Americans falls ill due to foodborne diseases and 3,000 die (CDC, 2018). In addition, food contamination imposes over $15.5 billion economic burden annually due to productivity losses, medical treatments, and hospitalizations (Hoffman, Maculloch & Batz, 2015).

Foodborne illnesses are caused by more than 40 different pathogens and over 95 percent are contributed to the following 15 pathogens: *Campylobacter* spp., *Clostridium perfringens*, *Cryptosporidium* spp., *Cyclospora cayetanensis*, *Listeria monocytogenes*, Norovirus, *Salmonella* non-typhoidal species, *Shigella* spp., STEC O157, STEC non-O157, *Toxoplasma gondii*, *Vibrio vulnificus*, *Vibrio parahaemolyticus, Vibrio* other non-cholera species, and *Yersinia enterocolitica* (Hoffman et al., 2015). In addition, the leading causes of death were nontyphoidal *Salmonella* spp.,

Toxoplasma gondii, *L. monocytogenes*, and norovirus (Scallan et al., 2011). The risk of foodborne illness has increased significantly and preventing foodborne illness still remains as a challenging field.

2.1.2. Conventional detection methods

The standard practice to ensure food safety and quality is to screen food products for the presence of both pathogenic and spoilage bacteria. Food safety screening relies on culture and colony counting, immunology-based, biochemical, and genetic analysis methods (de Boer & Beumer, 1999).

Conventional culture method, which relies on the growth of a single cell into a colony, is the standard microbiological technique for the detection of foodborne pathogenic bacteria (Velusamy et al., 2010). It involves multiple steps such as pre-enrichment, selective enrichment, biochemical screening, and serological confirmation (de Boer & Beumer, 1999; Zhao et al., 2014). This culture method has been validated to be highly sensitive, reliable, and inexpensive; however, being laborious and time-consuming as it takes 2-3 days to obtain initial results and up to 7-10 days for confirmation. Additionally, pathogens in the state of viable dormancy but not culturable can lead to underestimation of the pathogen and yield inaccurate results (Ahmed et al., 2014; Harrigan., 1998; Velusamy et al., 2010). Therefore, this technique is inadequate to meet the demand for rapid and accurate detection of foodborne pathogens.

Immunological detection methods are based on the specific binding of an antibody to an antigen (Zhao et al., 2014). One of the most widely used immunological assays is enzyme-linked immunosorbent assay (ELISA) (Ahmed et al., 2014). ELISA produces observable color changes to indicate the presence of antigens by employing chromogenic reporters and substrates. Among many ELISA methods, the sandwich ELISA is the most powerful kit as it binds the target antigen

between two antibodies: the primary antibody and the enzyme-conjugated antibody. The primary antibody is fixed onto a solid support and the target antigen binds to the primary antibody. The enzyme-conjugated secondary antibody reacts with the antigen and produces enzyme-mediated color change reaction as a signal (Zhang, 2013; Zhao et al., 2014). One of the main drawbacks of ELISA is a low sensitivity (10^4 - 10^5 CFU/mL) (Mandal et al., 2011). Feng et al. (2013) developed a monoclonal antibody-based ELISA for the detection of *E. coli* O157:H7 and achieved sensitivity of 10^4 CFU/mL. In order to improve the sensitivity, ELISA was coupled with other methods such as immunomagnetic separation and flow cytometry. Wang et al. (2013) tested the immunomagnetic separation technique combined with ELISA to detect *Alicyclobacillus* spp. in apple juice and the reported limit of detection (LOD) was 10^3 CFU/mL. Although these assays have enhanced the sensitivity, they are inappropriate for industrial needs as they require optical instruments and time-consuming sample enrichment step.

The nucleic acid-based assay detects the target pathogens by probing for specific DNA or RNA sequences. Current nucleic acid-based methods rely on the polymerase chain reaction (PCR) (de Boer & Beumer, 1999; Velusamy et al., 2010; Zhao et al., 2014). PCR relies on the amplification of target DNA or RNA segments by repetitive cycles of strand denaturation, annealing, and extension of primers by a thermo-stable polymerase enzyme (Leonard et al., 2003; Sharma & Mutharasan, 2013). The target nucleic segment is amplified 1-million-fold in less than an hour and the quantity of the nucleic segment can be visualized as a band on an ethidium bromide-stained electrophoresis gel (de Boer & Beumer, 1999). Some advantages of PCR are high sensitivity and rapidity as it does not require a bacterial culture step (Ahmed et al., 2014; Velusamy et al., 2010). However, PCR techniques have major limitations such as the occurrence of false-negative results due to the interference from food samples and inability to distinguish between live

and dead cells (de Boer & Beumer, 1999; Zhang, 2013). To overcome these limitations, a wide range of PCR based methods such as real-time PCR, multiplex PCR, and quantitative PCR have been developed (Choi & Lee, 2004; Kawasaki et al., 2009; Malorny et al., 2004; Zhao et al., 2014). Timmons et al. (2013) fabricated a multiplex assay to simultaneously detect *Salmonella enterica* Typhimurium and *E. coli* O157:H7 in fresh tomato and jalapeño pepper washes and was able to detect between 10 to 10^2 CFU/ mL from the washes. Nam et al. (2005) developed a real-time PCR to detect *Salmonella* spp. and achieved a detection range between 10^3 to 10^4 CFU/mL without enrichment and <10 CFU/mL with 18 h enrichment. Hsu, Tsai & Pan (2005) used a real-time PCR to detect 10^3 to 10^9 CFU/mL of *E. coli* O157:H7 in pure culture and milk samples and 10^4 to 10^9 in apple juice. Kim et al. (2012) investigated the use of a multiplex rea-time PCR to detect *Vibrio cholerae*, *V. parahaemolyticus*, and *V. vulnificus* and observed a LOD of 10^0 CFU/g in seafood homogenate with 8 h enrichment. Despite of its low sensitivity and specificity, PCR is expensive, requires skilled personnel, and a lab-based equipment.

Due to these limitations, there is a real need for rapid, sensitive, and simple detection methods that can be deployed for on-site monitoring.

2.1.3. Biosensors for detection of foodborne pathogens

The biosensor is an analytical device which translates a specific bio-recognition event into a measurable signal. It is composed of a bioreceptor, which couples with the target analyte, and a transducer to convert the recognition event into a detectable signal (Ahmed et al., 2014; Singh, Poshtiban & Evoy, 2013). Some advantages of biosensors are high sensitivity and specificity, cost-

effectiveness, miniaturization, portability, and reduced overall required time (Ahmed et al., 2014). Biosensors can be classified according to their bioreceptor or their transducer types (Figure 2.1).

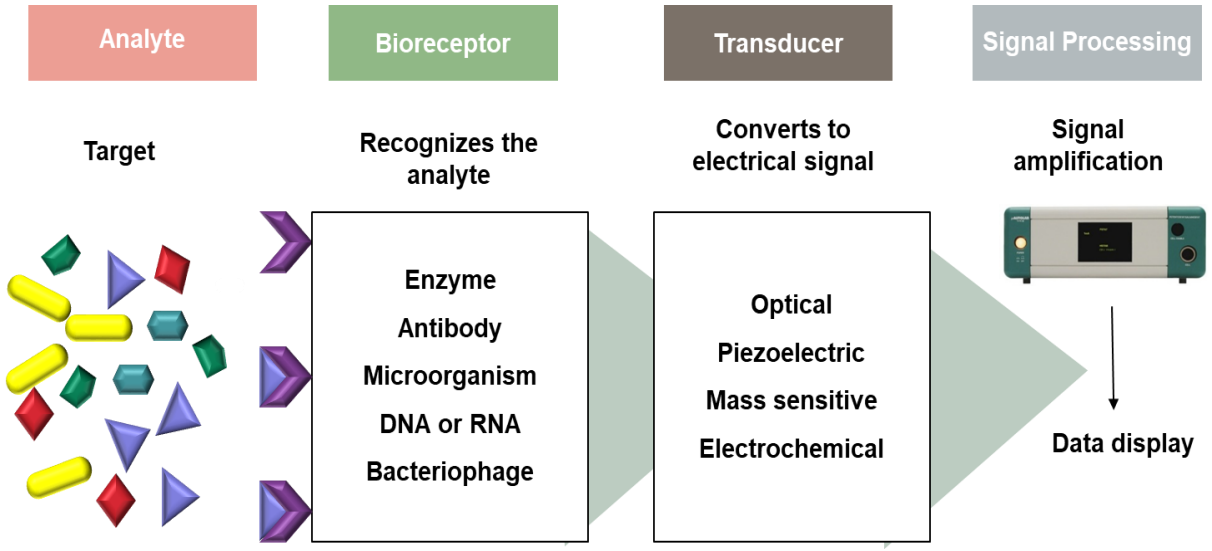

Figure 2.1. Common classifications of biosensor.

The performance of a biosensor is highly dependent on the sensing capability of the incorporated bioreceptor. Enzymatic biosensors are capable of providing rapid responses. Their main drawback is high production cost and variability in their performance. An aptamer-based biosensors are suitable for the recognition of small molecules as well as bacterial cells. However, their main limitation is their commercial development is still in its infancy (Gaudin, 2017). Antibody is a commonly used bioreceptor due to their high specificity, stability, and strong affinity for the antigen (Velusamy et al., 2010). Antibodies correspond to an antigen in a highly specific manner, similar to a lock and key fit. Based on the synthesis method, antibodies can be polyclonal, monoclonal or recombinant. In addition, they can be labeled with enzymes, biotin, fluorophores, and radioactive isotopes to enhance the detection signal (Conroy et al., 2009).

The most commonly used transduction methods are electrochemical, mass, and optical-based methods due to their sensitivity and simplicity (Velusamy et al., 2010). Optical biosensors

utilize changes in the optical properties of the sensor surface and these are transduced by a detector. These sensors are classified into subclasses based on the measure of absorption, reflection, refraction, infrared, and fluorescence (Ahmed et al., 2014). Wang et al. (2011) demonstrated that an SPR-based immunosensor achieved a LOD of 3.0×10^4 CFU/mL for the detection of *E. coli* O157:H7. Taylor et al. (2006) developed a multi-channel SPR biosensor for the simultaneous detection of multiple target analytes including *E. coli* O157:H7, *Salmonella choleraesuis serotype typhimurium, L. monocytogenes*, and *C. jejuni* and detected 3.4×10^4 to 1.2×10^5 CFU/mL. Despite the high sensitivity and specificity, optical biosensors are not suitable for industrial application as they must be equipped with complex instrument including a suitable spectrometer, fiberoptics, laser, prism, and waveguides (Zhao et al., 2014).

Mass-sensitive biosensors is based on measuring the small changes in mass. Binding of the target results in an increase in mass and changes the oscillation frequency of the piezoelectric crystals (Sharma & Mutharasan, 2013; Velusamy et al., 2010). Si et al. (2001) reported a quartz crystal microbalance sensor for the detection of *Salmonella enteritidis* with a detection limit of 10^5 CFU/mL within 35 min. Wong et al. (2002) produced a quartz crystal microbalance sensor that distinguished *Salmonella* spp. from other serogroups with a LOD of 10^4 CFU/mL. Although this technology is simple, it is not commonly used for the detection of foodborne pathogens.

2.1.3.1. Electrochemical impedimetric biosensor

Electrochemical biosensors respond to a biological recognition event on the surface of the sensor by means of an electrochemical method. They are classified into amperometric, potentiometric, and impedimetric based on the measured parameter such as current, potential, and impedance (Sharma & Mutharasan, 2013; Velusamy et al., 2010). Impedimetric biosensor is a promising method for the detection of bacteria due to its portability, rapidity, sensitivity, and cost

efficiency (Ahmed et al., 2014; Prodromidis, 2010; Wang et al., 2012). Impedance is defined as the apparent resistance in an electric circuit to the flow of alternating current (Sharma & Mutharasan, 2013). In the presence of a redox probe ($[Fe(CN)_6]^{3-/4-}$), a bacterial cell bound to a transducer surface causes a decrease in an electron transfer current (Figure 2.2 (a)). According to the equation 2.1, the ratio of the voltage-time function V(t) and the resulting current-time function I(t) is the impedance of an electrode.

$$Z = \frac{V(t)}{I(t)} = \frac{1}{Y} = \frac{V_0 \sin(2\pi f t)}{I_0 \sin(2\pi f t + \varphi)} \quad (2.1)$$

V_0 and I_0 are the maximum voltage and current signals, f is the frequency, t is time, φ is the phase shift between the voltage-time and current-time functions, and Y is the complex conductance or admittance. Impedance is determined by employing a technique called Electrochemical Impedance Spectroscopy (EIS). EIS describes the response of an electrochemical cell to a small amplitude sinusoidal voltage signal as a function of frequency (Sharma & Mutharasan, 2013; Wang et al., 2012). EIS data are commonly displayed using a Nyquist plot, which plots the imaginary impedance component (Z``) against the real impedance component (Z`) as presented in Figure 2.2 (b). A typical shape of a Nyquist plot includes a semicircle region lying on the real axis followed by a straight line. At high frequency, impedance arises from the electrolyte solution itself, whereas at lower frequency, impedance results from the resistance to the flow of electrons to the electrode surface. The Nyquist plot is translated into an equivalent circuit model, Randles circuit, to investigate the electrical parameters including the electron transfer resistance (R_{et}) (Figure 2.2 (c)).The R_{et} is an important parameter in analyzing the impedance changes of a sensor. In the presence of a redox probe, a biorecognition event on the sensing platform reduces the electron

transfer across the surface and the R_{et} is altered (Lisdat & Schäfer, 2008). Impedimetric immunosensor which detects foodborne pathogens by immobilizing antibodies on the surface of a transducer has been widely used. Dweik et al. (2012) fabricated an impedance biosensor for the detection of *E. coli* O157:H7 with a LOD of 2.5×10^4 CFU/mL. Huang et al. (2010) detected 1.0×10^3 to 1.0×10^7 CFU/mL of *Campylobacter jejuni* using an electrochemical impedimetric immunosensor. Although the impedimetric immunosensor is considered a promising candidate for the detection of foodborne pathogens, it still has some main areas to improve such as enhancing the sensitivity and immobilization of antibodies on the transducer surface.

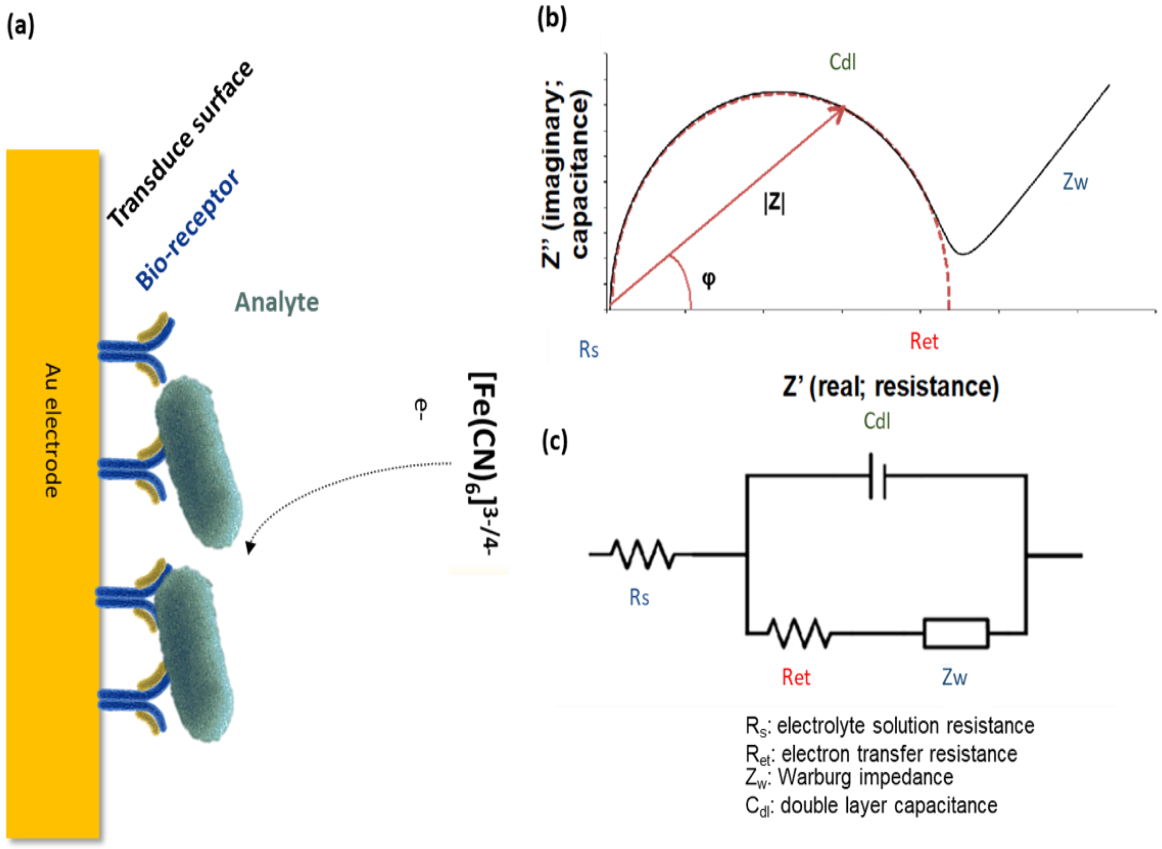

Figure 2.2. A schematic and principle of the impedance measurement. (a) A sensing surface compromising of a receptor attached on the electrode. The exchange of electrons between the redox probe is reduced due to the barrier generated by the receptive film and bound target (b) The Nyquist plot (Zim vs Zre) in the presence of redox probe $[Fe(CN)6]^{3-/4-}$. (c) Randles equivalent circuit to fit the Nyquist plot.

2.1.3.2. Nanomaterials for sensing element

Introducing nanomaterials is a promising method to enhance the performance of biosensors. Nanomaterials are defined as a set of materials having at least one dimension less than 100 nanometer. Their unique physicochemical properties have potential to offer substantial advantages for biosensing. For example, their properties such as chemical and thermal stability, high elasticity, and high tensile strength can improve the sensitivity and stability of the biosensor (Holzinger et al., 2014; Wang et al., 2012). Among the nanomaterials, nanoparticles, nanowires, and carbon nanotubes have been utilized for the detection of bacteria with enhanced analytical performance (Wan et al., 2010; Wang et al., 2008; Yun et al., 2007). Examples of nanomaterials-based biosensors are listed in Table 2.1.

Table 2.1 Nanomaterials-based biosensors for the foodborne pathogen detection

Type	Pathogens	Nanomaterials	Assay time	LOD (CFU/mL)	Reference
Electrochemical	*Salmonella*	SWCNT	4 h	1.6×10^4	(Jain et al., 2012)
	E. coli K12	SWCNT	5 min	10^2	(Yamada et al., 2014)
	L. monocytogenes	TiO2 nanowire	50 min	4.7×10^2	(Wang et al., 2008)
Colorimetric	*E. coli* O157:H7	AuNPs	1 h	50	(Zheng et al., 2019)
	E. coli O157:H7	AuNPs	95min	41	(Xu et al., 2017)
	E. coli O157:H7	AuNPs	45min	10^2	(Ren et al., 2019)
Fluorescence	*S. enterica*	CdTe	2 h	5×10^2	(Wang et al., 2015)
	S. enteritidis	CdTe	2 h	10^3	(Shi et al., 2015)
	E. coli O157: H7	QD and IMBs	1 h	1.5×10^3	(Yin et al., 2016)
SERS	*S. aureus*	AuNFs	40 s	10^3	(Juneja & Bhattacharya, 2019)
	E. coli and *S. epidermidis*	AgNPs	10 min	2.5×10^2	(Zhou et al., 2014)

2.1.3.3. Integration of single-walled carbon nanotubes for biosensing

Among the many nanomaterials, carbon nanotubes have been extensively studied due to their electrical, chemical, mechanical, and structural properties (Allen, Kichambare & Star, 2007). Carbon nanotubes are sp^2 carbons arranged in graphene sheets rolled-up to form a hollow tube. They can be divided into a single-walled carbon nanotube (SWCNT) and a multi-walled carbon nanotubes (MWCNT). The diameters of SWCNTs range from 0.4 nm to 3 nm. The MWCNTs are composed of multiple graphene tubes with a 0.34 nm interlayer gap and the diameter varies from 1.4 nm to 100 nm. SWCNTs are particularly attractive as they exhibit excellent conductivity, high chemical stability, and sensitivity to environmental changes as every atom is exposed to the surrounding (Allen et al., 2007; Trojanowicz, 2006). They can be metallic or semi-conductors depending on their diameter and chirality. The chirality is related to the angle at which the graphene sheets are rolled up. The angle is described by a vector lattice with integers (*n, m*). The metallic nanotubes are achiral with arm-chair configuration with indices (*n, n*), while semi-conducting nanotubes are chiral (*n, m*) and achiral zig-zag (*n*, 0) (Figure 2.3).

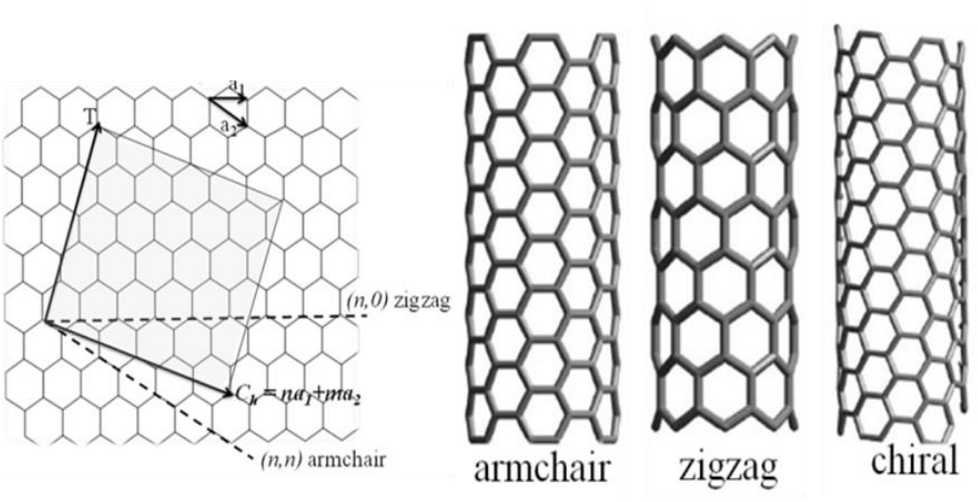

Figure 2.3. SWCNT armchair, chiral, and zig-zag forms (Odom et al., 2000).

There are three main methods of CNT syntesis: arc-discharge, laser-ablation, and chemical vapor deposition. Arc-discharge is the growth of CNTS on graphite electrodes. It involves a direct current between a pair of graphite electrodes under an inert gas such as helium or argon. Although CNTs synthesized by arc discharge show a high degree of structural perfection, variables such as temperature, the presence of hydrogen, and the concentration of catalyst influence their size and structure. Laser-ablation method involves vaporizing a target consisting of a mixture of graphite and metal catalysts in the presence of helium or argon gas by a laser beam pulse at high temperatures (800 - 1500°C). Variables such as chemical composition of the target material, wavelength and power of the laser, and distance between the target and the substrates affect the quantity of CNTS produced. Chemicval vapor deposition promotes the growth of nanotubes by heating a gaseous hydrocarbon source to 600 - 1000°C with a transition metal catalyst. CVD allows mass production with the control over diameter and shell number. However, higher defect density is observed with this method when compared with the other two methods (Ferreira et al., 2019).

In biosensing, SWCNTs can offer many advantages. SWCNTs have a large specific surface area which enables immobilization of a large number of bioreceptors such as proteins, enzymes, antigens, antibodies or DNA. In addition, their ability to enhance the electron transfer and transduce the electrical signals generated upon the recognition of a target make them suitable for a wide range of biosensors (Sireesha et al., 2018). Zhou, Wang & Chang (2006) detected 10^4 CFU/mL of *E. coli* by applying dielectrophoresis force using SWCNTs. Yoo et al. (2016) functionalized SWCNT-FET with DNA probes using covalent reaction and selectively detected *S. aureus* and *E. coli* with a LOD of 10 CFU/mL. Yoo et al. (2017) fabricated SWCNTs-based electrochemical biosensor for the detection of *Bacillus subtilis* and detected 10^2 - 10^{10} CFU/mL range within 10 min. One of the major limitations of conjugating SWCNTs into biosensors is their

hydrophobic nature. The ends of the SWCNTs are hydrophilic as they are terminated in oxygenated species and the walls are highly hydrophobic. Therefore, they tend to spontaneously coagulate in almost all kinds of aqueous and organic solutions (Odom et al., 2000). As a consequence, the SWCNTs undergo modifications to achieve aqueous dispersion and solubilization. One of the common methods is treatment with oxidative acid such as refluxing and sonicating in a concentrated mixture of sulfuric and nitric acid. This procedure produces carboxylated sites on the SWCNT walls and allows them to adsorb onto the electrode surface. Kam & Dai (2005) produced -COOH groups on SWCNTs by refluxing and sonicating them in nitric acid and they were found to be stable in aqueous solutions. Although this procedure is effective in producing functional groups, it can produce defects on the surface of SWCNTs and impair the desirable mechanical and electronic properties (Allen et al., 2007; Putzbach & Ronkainen, 2013). Another approach to disperse SWCNTs is a non-covalent method. This procedure involves ultrasonication, centrifugation, or filtration in either surfactant or non-polar organic solvents such as N, N-dimethylformamide (DMF) (Lin et al., 2004). This method is known to be non-destructive and preserves the nanotube structures and their unique properties (Allen et al., 2007). Kang & Taton (2003) dispersed SWCNTs in amphiphilic deblock polymer and cross-liked the hydrophilic outer shell of the micelle with polyacrylic acid. Lee et al. (2008) used DMF to disperse SWCNT powder and achieved uniformly separated suspension.

2.2. Nanoengineered surfaces to control bacterial adhesion and biofilm formation

Bacterial adhesion on food-contact surfaces is a major problem in the food industry. It has been shown that bacterial cell attachment depends highly on the micro/nanostructures of the substrate. Therefore, nanotechnology has been extensively explored to produce anti-biofouling surfaces by altering the surface properties.

2.2.1. Significance of biofouling in the food industry

Biofouling refers to the undesirable microbial adhesion, followed by the build-up of biofilms. Biofilms are defined as communities of surface-associated microbial cells that are enclosed in hydrated extracellular polymeric substances (EPS) (Kumar & Anand, 1998; Sauer, Rickard & Davies, 2007). In the food processing environment, conditions such as flowing water, suitable attachment surfaces, and available nutrients favor bio-adhesion and biofilm formation (Gibson et al., 1999). As a result, a variety of bacteria and biofilms have been isolated from food-contact surfaces including pathogenic microorganisms such as *L. monocytogenes*, *Yersinia enterocolitica*, *Campylobacter jejuni*, and *E. coli* O157:H7 (Frank & Koffi, 1990; Herald & Zottola, 1988; Kuusela et al., 1989; Shi & Zhu, 2009). Bacteria dispersed from biofilms are a major source of end-product contamination or transmission of diseases. In addition, biofilm layers can cause heat transfer impedance, reduce production efficiency, and equipment failure as well (Garrett, Bhakoo & Zhang, 2008; Sandu & Singh, 1991).

Bacterial cells enclosed in biofilms behave differently from their planktonic counterparts, especially in terms of their response to biocides. For instance, *Salmonella* in biofilms were more resistant to trisodium phosphate, chlorine, and iodine than their planktonic cells (Joseph et al., 2001; Scher, Romling & Yaron, 2005). *L. monocytogenes* enclosed in biofilms were highly resistant to various anti-microbials including trisodium phosphate, chlorine, ozone, hydrogen peroxide, peracetic acid, and quaternary ammonium compounds (Frank & Koffi, 1990; Lee & Frank, 1991; Somers, Schoeni & Wong, 1994; Van Houdt & Michiels, 2010). This observed response could be due to the altered physiological state of the bacteria, resulting in a decreased growth rate and starvation responses. In addition, the intricate structure of biofilms with EPS

results in a low diffusion of the antibiotics reaching the bacteria (Van Houdt & Michiels, 2010). Therefore, there is a great demand for developing a novel anti-biofilm agent for the food industry.

2.2.2. Conventional strategies to prevent biofouling

The main strategy to prevent biofilm formation is to clean and disinfect regularly before biofilms are established on food-contact surfaces (Chmielewski & Frank, 2003; Kumar & Anand, 1998; Møretrø & Langsrud, 2004). Most cleaning agents used in the food processing industries are alkali or acid compounds (Srey, Jahid & Ha, 2013). The main drawback of these standard compounds is the insufficient removal of microorganisms (approximately 90%) from surfaces due to the virtue of their complex structure. Gibson et al. (1999) observed that alkali and acid cleaners only resulted in 1-log reduction of *Pseudomonas* and *S. aureus* enclosed in biofilms. In addition, cleaning may result in aerosol generation which could disperse microorganisms over an extensive area and produce a novel biofilm. Therefore, chemical disinfectants including chlorine, hydrogen peroxide, iodine, peracetic acid, and quaternary ammonium compounds are commonly used in the food industry (Akbas, 2015; Van Houdt & Michiels, 2010). However, their efficacy is greatly influenced by the presence of organic material (fat, carbohydrates, protein), pH, temperature, contact time, and chemical inhibitors (Simões et al., 2010). Norwood & Gilmour (2000) reported that active chlorine concentration of 1,000 ppm was needed to obtain significant reduction of bacterial cells in a biofilm, whereas 100 ppm was sufficient for planktonic cells. Keskinen, Burke & Annous (2009) achieved 1-log CFU/g reduction of *E. coli* O157:H7 on fresh-cut leaves with a chlorine treatment (20 - 200 ppm). As an alternative to these chemical disinfectants, other treatments have been extensively studied. Electrical methods such as electric field, ultrasound, and ultrasonication have been investigated to enhance biofilm removal and have shown to be limited to small areas (Meyer, 2003). Automatic scrubber or high-pressure cleaning, which utilizes

mechanical force was also investigated. Unfortunately, these methods can also spread the surviving microbes via aerosols and elevate hygiene problems (Gibson et al., 1999).

In addition to cleaning, food-contact surfaces are hygienically designed to prevent the accumulation and transfer of contaminants. For example, dead spaces and corners are either removed or well radiused to prevent the establishment of microorganisms and product residues. Joints and fasteners are avoided or crevice-free to provide a smooth continuous surface for cleaning (Lelieveld, Mostert & Curiel, 2014). Despite the good hygienic practices, bacterial adhesion is difficult to avoid as it is a fast process and it has been reported that microorganisms can colonize on materials commonly found in the food processing environment i.e. glass, polytetrafluoroethylene, stainless steel, plastics, and rubber (Akbas, 2015; Brooks & Flint, 2008; Shi & Zhu, 2009). Therefore, there is a need to develop anti-bacterial and anti-biofilm materials.

2.2.3. Superhydrophobic biofouling resistant surfaces

It has been shown that the material design and surface engineering could reduce biofouling by governing bacterial adhesion on substrates. In most cases, the anti-biofouling performance is chiefly determined by the surface physical and chemical properties. Gillett et al. (2016) modified PET coupons with a laser treatment to enhance the hydrophobicity and observed a 10-fold reduction in the number of attached *E. coli* cells. Yang et al. (2010) modified the microporous polypropylene membrane by UV to induce surface hydrophilicity (WCA decreased from 145° to 15°) and observed a reduction in the adhesion of *S. aureus* by 97%. Among many surface modifications, superhydrophobic (SH) surface has gained a significant interest due to their unique properties and potential applications in various fields. SH surface, inspired by the Lotus leaf in nature, is extremely non-wettable and can be fabricated by introducing low surface energy micro/nanoscale roughness (Gu & Ren, 2014; Zhang, Wang & Levänen, 2013). SH surface has

shown to prevent the surface biocontamination by reducing the contact area between the droplet and the solid surface. Other well-known functionalities of SH surface are water repellency, anti-icing, anti-reflecting, non-adhesive property (Cao et al., 2009; Nosonovsky & Bhushan, 2008; Zhang et al., 2008; Zhang et al., 2013).

2.2.3.1. Designing superhydrophobic surfaces

Wetting on a flat surface

The surface wettability of a liquid droplet deposited on a chemically homogeneous and physically smooth solid surface is mainly determined by the surface chemical composition. The WCA on a smooth surface is defined by the Young's equation as follows:

$$\cos\theta_Y = \frac{\gamma_{SV} - \gamma_{SL}}{\gamma_{LV}} \qquad (2.2)$$

γ_{SV} is the solid surface energy, γ_{SL} is the solid-liquid interfacial energy, and γ_{LV} is the liquid surface tension. The WCA is defined as the angle between the tangent to the liquid-vapor interface and the tangent to the liquid-solid interface at the contact line between the three phases (Figure 2.4). According to the Young's equation, the surface hydrophobicity increases with decreasing the γ_{SV}. A surface is regarded as hydrophobic with a WCA greater than 90° and below 90° is considered as hydrophilic. It has been reported that the WCA of a surface with the lowest γ_{SV} on a non-textured surface is about 130° (Öner & McCarthy, 2000; Marmur, 2003). Therefore, manipulation of the surface topography is required for further enhance the surface hydrophobicity.

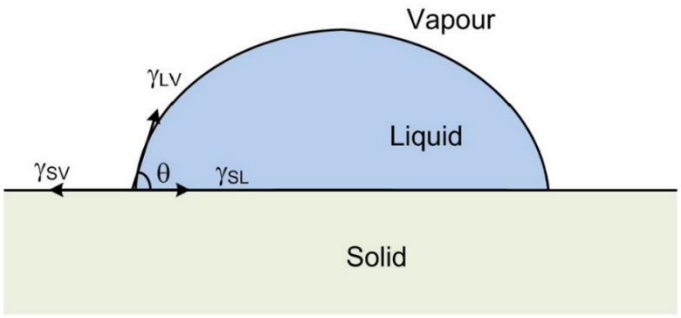

Figure 2.4. A schematic of a water drop on smooth surface.

Wetting on a textured surface

A liquid droplet on a textured surface is described as a Wenzel state or Cassie-Baxter state. In the Wenzel state, the droplet penetrates the texture and wets the surface thoroughly (Figure 2.5 (a)). The apparent contact angle in the Wenzel state is predicted by:

$$\cos\theta_W = r_s \cos\theta \qquad (2.3)$$

where r_s is the roughness factor defined as the ratio of actual surface area to the geometric surface area. Since r_s is always greater than 1 for a rough surface, based on the Wenzel equation, a surface with $\theta_W > 90°$ displays $\theta_W > \theta > 90°$ and a surface with $\theta_W < 90°$ displays $\theta_W < \theta < 90°$. Therefore, in the Wenzel state, surface roughness increases the hydrophobicity of a hydrophobic surface and hydrophilicity of a hydrophilic surface. As the surface roughness increases, air may be trapped between the water and the surface texture. As a result, liquid is in contact with a composite surface of solid and air, and thus, forms droplets. This state is called the Cassie-Baxter state. The apparent contact angle θ_c for a droplet in the Cassie-Baxter is given by:

$$\cos\theta_c = f_1 \cos\theta_y - f_2 \qquad (2.4)$$

where f_1 and f_2 are the air and surface fraction, respectively, and θ_c is the modified apparent contact angle due to the porous surfaces (Figure 2.5 (b)). Air entrapment will form air porckets and remarkably increase the apparent surface hydrophobicity. Based on the Cassie-Baxter equation, a decrease of f_2 results in an increase of θ_c and eventually leads to a superhydrophobic state. The WCA of a superhydrophobic surface is greater than 150° and a sliding angle is less than 10° (Gu & Ren, 2014; Mohamed, Abdullah & Younan, 2015; Zhang et al., 2013). The water droplet on this surface does not completely infiltrate the rough surface since air is entrapped in the groove. Therefore, the contact area between the droplet and the solid surface is reduced.

The WCA of the surface is usually measured by dispensing a drop onto the surface, known as a quasi-static deposition. On the SH surface, the quasi-static deposition will transition from the Cassie to the Wenzel state when the energy barrier between the two states is overcome by external factors such as the pressure of the drop, the drop size, and gravity (Patankar, 2004; Zhang et al., 2013). According to Patankar (2004), the barrier energy can be estimated by measuring the maximum energy state within the intermediate stage. In addition, the water drop should be smaller than 82 mg to minimize the effects of the gravity in determining the Cassie and Wenzel states (Patankar, 2004). According to Sarkar & Kietzig (2015), the intermediate partial liquid penetration, termed as a metastable Cassie state, occurs by sag and depinning mechanisms. In the sag mechanism, the apex of the roughness valleys pins the liquid and a part of the liquid-air interface sags due to the gravitational force. In the depinning mechanism, the gravitional force acting on the solid-liquid interface is greater than the shear force and the solid-liquid contact gets de-pinned from the rough surface. The preferred Cassie-Baxter state is produced when the surface energy of a material is more favorable in comparison to the Wenzel state. The Wenzel state surface exhibits both sag and depinning transitions. Regardless of the surface geometry, it is postulated that the

quasi-statically robust superhydrophobic surface should withstand a minimum antiwetting pressure of 117 Pa and impact velocity less than 100 mm/s.

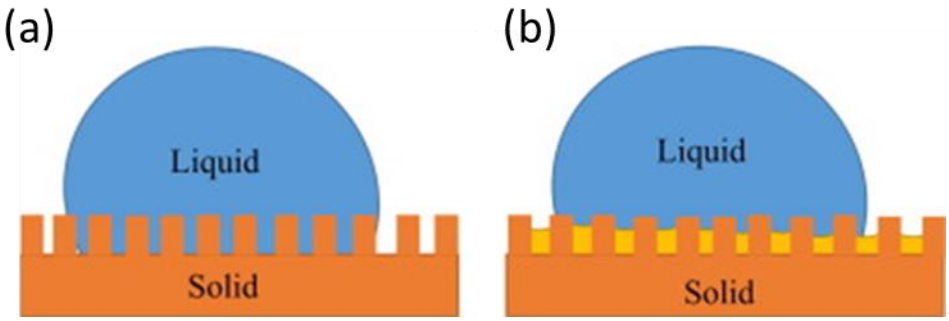

Figure 2.5. A schematic of a liquid drop in the (a) Wenzel state (b) Cassie-Baxter state.

2.2.3.2. Nanostructures to fabricate superhydrophobic anti-biofouling surface

Nanostructures on a solid surface are essential to produce a SH surface. As explained by the Cassie-Baxter equation, the nanostructures enhance the surface roughness and yield a large WCA. Advances in nanotechnology have stimulated the development of SH surfaces on various substrates. Liu et al. (2015) developed a SH stainless steel by chemical etching to obtain nanoscale roughness and observed WCA of 158.3° ± 2.8°. Kamegawa, Shimizu & Yamashita (2012) produced a nanocomposite coating of TiO_2 and PTFE and the film exhibited WCA of 168°. Boinovich et al. (2013) fabricated a SH surface on stainless steel (WCA > 155°) with silica nanoparticles by chemical etching and dispersion. Sun et al. (2005) developed a SH film on a poly (carbonate urethane) by coating with fluorinated alkyl side chains and carbon nanotubes and achieved WCA > 163°.

The SH surface is a promising tool to minimize microbial adhesion on substrates (Table 2.2). The anti-bacterial activity of the SHc surfaces could be attributed to the decreased contact area between the bacteria and the surface, resulting in a low binding strength. Privett et al. (2011)

synthesized a SH (WCA ≈ 167°) xerogel from a mixture of nanostructured fluorinated silica colloids and demonstrated that the adhesion of *S. aureus* and *P. aeruginosa* were reduced by 2.08 ± 0.25 and 1.76 ± 0.12 log, respectively. Crick et al. (2011) reported SH surface made from a silicone elastomer via an aerosol assisted chemical vapor deposition process. The film had WCA averaging 165° and the adherence of *E. coli* and *S. aureus* were reduced by 58% and 79%, respectively (Crick et al., 2011). Freschau et al. (2012) conducted a structural modification by multi-scale metal-coated shrink film to fabricate a SH surface (WCA ≈ 150° - 167°) on hard plastics and observed the reduction in the adhesion of *E. coli* by 98%. Pernites et al. (2011) prepared a SH polymeric surface by layering polystyrene latex particles and electrodeposition of polythiophene. The surface demonstrated WCA 152° ± 3° and reduction in the adhesion of fibrinogen proteins and *E. coli* cells (Pernites et al., 2011).

Table 2.2. Bacterial adhesion on superhydrophobic surfaces

Bacterium	Processing	Contact angle (°)	Reduction (%)	Reference
Stahylococcus aureus *Pseudomonoas aeruginosa*	Fluorinated silica colloids	167	99 98	(Privett et al., 2011)
Staohylococcus aureus *Escherichia coli*	Aerosol assisted chemical vapour deposition	165	58 79	(Crick et al., 2011)
Escherichia coli	Shrink-wrap film	150 - 167	98	(Freschau et al., 2012)
Staphylococcus aureus *Escherichia coli*	Anodizing and postetching with Teflon	162	99.9 99.4	(Hizal et al., 2017)
Escherichia coli	Hydrothermal	155	87.5	(Wang et al., 2015)

2.2.3.3. Fabrication of superhydrophobic surface via electrochemical etching and Teflon

Electrochemical etching

Since the electrochemical etching was suggested by Tommasino in 1970, this method has been widely used for decades. The electrochemical etching is known as the anodization approach which uses electrochemical erosion to remove metals. In the electrochemical etching, the active metal acts as an anode (+) and the noble metal acts as a cathode (-). Both metals are immersed inside an electrolyte solution and the active metal is oxidized by the removal of bonding electrons via an external voltage source (Ahmad, 2006; Zhuang & Edgar, 2005). During electrochemical etching, the most important process is the formation of a track or track pit as shown in Figure 2.6. A track is enlarged when the speed of etching along the track, V_T, is greater than the speed of etching along the surface, V_S (Durrani & Bull, 2013). The surface etching rate is related to the morphological structure of the material as the chemical reagent must diffuse to the material. Contrast to chemical etching, the application of electrical stresses enhances the penetration of the etchant into the surface (Durrani & Bull, 2013).

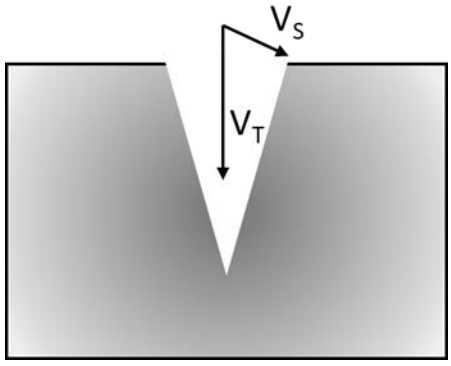

Figure 2.6. The basic mechanism of electrochemical etching (Durrani & Bull, 2013).

Stainless steel is a material commonly found in the food industry due to its beneficial properties such as corrosion resistance, inertness of surface, and resistance to wide range of temperatures (Cvetkovski, 2012). It is an alloy composed of several elements including iron (Chen et al., 2005). In an electrochemical cell, stainless steel serves as an anode and a carbon plate is usually used as a counter electrode. As etchants, HCl and HNO_3 are widely used to form uniform spreading of pits on the stainless steel are. During the electrochemical reaction, Cl^- anions create nucleation sites and NO_3^- anions allow the formation of even pits (Jeżowski et al., 2015; Lee & Shih, 1996). Although the entire process has not been fully understood yet, iron present in stainless steel reacts with HCl according to the following half-reactions:

$$Fe \rightarrow Fe^{2+} + 2e^- \quad (2.5)$$

$$2H^+ + 2e^- \rightarrow H_2 \quad (2.6)$$

Sum of the above half-reactions:

$$Fe + 2H^+ \rightarrow Fe^{2+} + H_2 \quad (2.7)$$

Iron is oxidized to form ferrous ions and hydrogen ions are reduced to hydrogen gas. When the two electrodes are not electrically connected, the overall reaction will not occur since the half-reactions are at equilibrium. When external power is applied, electrons flow from the anode to the cathode and initiate the electrochemical erosion (Kutz, 2018). The electrochemical parameters such as potential and current are important since they manipulate the surface roughness via controlling the nanopore diameters (Darmanin et al., 2013; Jang et al., 2017). In addition, the etching rate is affected by the presence of grain boundaries and matrices of the stainless steel as well (Figure 2.7). This is due to the presence of structural defects or variations in the alloy

composition at the grain boundaries, resulting in increased etch rates. Some of the advantages of electrochemical etching are affordable, scalable, and most importantly, have fine control of the surface structures (Darmanin et al., 2013; Jang et al., 2017).

Use of Teflon to reduce the surface energy

Polytetrafluoroethylene (PTFE), commercially named as Teflon, is a fluoropolymer material widely used in a variety of applications. It has a molecular formula [$(CF_2\text{-}CF_2)_n$] and possesses C-F bonds (Dhanumalayan & Joshi, 2018). The molecular structure of PTFE is shown in Figure 2.8. The C-F bond has high bonding energy, 116 kcal/mol, resulting in low surface energy (18 mN/m). Therefore, the water WCA on smooth PTFE surface is between 98° and 112°. PTFE has high thermal stability and chemical resistance as it requires high energy to break the C-F bond (Ebnesajjad, 2016; Lau et al., 2003). It is classified as thermoplastics as the average melting point is between 325 to 335°C. Figure 2.9 shows the unique properties of PTFE.

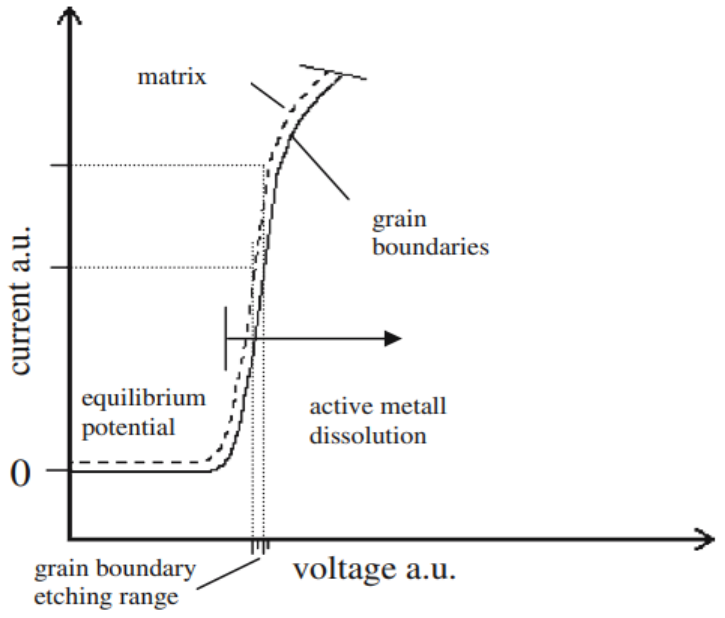

Figure 2.7. A current/voltage diagram to evaluate the ratio of grain boundary and matrix etch rate (Stöver et al., 2006).

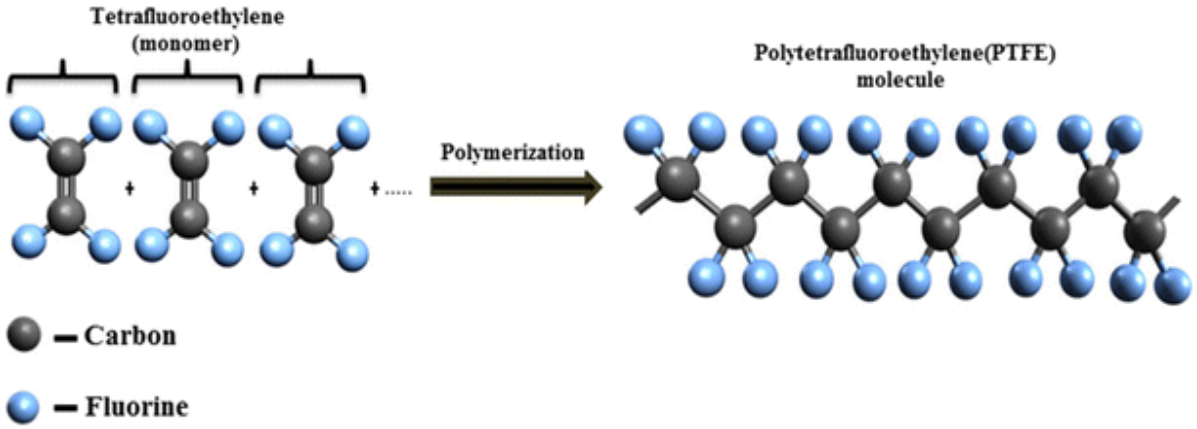

Figure 2.8. Polytetrafluoroethylene (PTFE) molecular structure (Dhanumalayan & Joshi, 2018).

In the food industry, PTFE is used from non-stick cookware surface coatings to the production of gaskets and packaging to restrict the adherence of other molecules over surfaces (Dhanumalayan & Joshi, 2018). The hydrophobic nature of PTFE is attributed to its low surface energy. Surface energy is a measure of work required to increase the surface area by unit area. It arises from molecules that are not fully interacting with other molecules and this leads to the production of free energy. As a consequence, these molecules at the surface interact with the adjacent phase to reduce the free energy. Therefore, a material of high surface energy, i.e. high bonding potential, interacts with water and exhibits hydrophilicity. Conversely, the opposite is observed with a low surface energy material. Therefore, the low surface energy material, PTFE can be used to reduce fouling, food contamination, and biofilm formation.

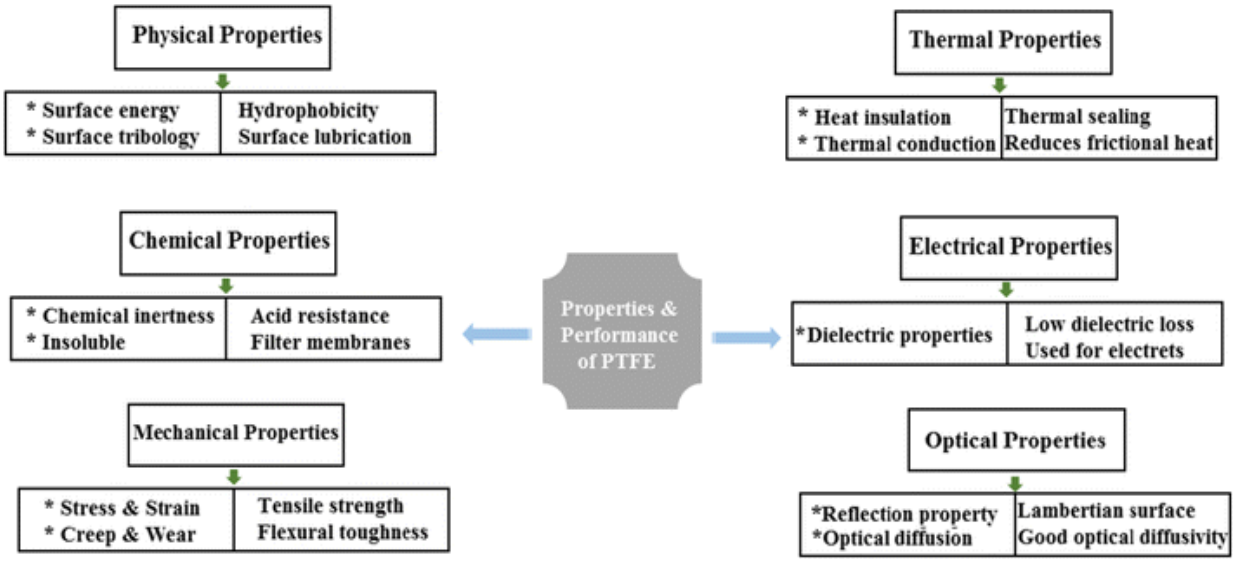

Figure 2.9. Properties and performance of PTFE (Dhanumalayan & Joshi, 2018).

2.3. Conclusion and thesis overview

Foodborne pathogens pose a serious threat to the food supply chain. Despite the advancement of many existing technologies, i.e. biosensing and bacterial resistant surfaces, foodborne illness outbreaks are difficult to overcome. Nanotechnology is a multidisciplinary field with promising applicability in various aspects within the food industry such as food safety and product development. This research investigated the application of nanotechnology, SWCNTs and nanoengineered surface, to improve food safety. The first part of this thesis studied the performance of a SWCNTs conjugated sensor by detecting *L. monocytogenes* in pure and microbial cocktail solutions. Based on the research findings, the sensor was integrated into a smartphone-controlled platform for field application. The second part of this thesis focused on the fabrication of nanoporous anti-bacterial surface by the combination of electrochemical etching and PTFE film. Results showed that the SWCNTs and nanoengineered surface significantly contributed to detecting a foodborne pathogen and minimizing the growth of biofilms.

Chapter 3.

A SWCNTS-BASED ELECTROCHEMICAL IMPEDANCE IMMUNOSENSOR FOR ON-SITE DETECTION OF *LISTERIA MONOCYTOGENES*

Abstract

Real-time and sensitive detection of pathogenic bacteria in food is in high demand to ensure food safety. In this study, a single-walled carbon nanotubes (SWCNTs)-based electrochemical impedance immunosensor for on-site detection of *Listeria monocytogenes* (*L. monocytogenes*) was developed. A gold plated tungsten wire was functionalized by coating with polyethylenimine, SWCNTs, streptavidin, biotinylated *L. monocytogenes* antibodies, and bovine serum albumin. A linear relationship (R^2 = 0.982) between the electron transfer resistance measurements and concentrations of *L. monocytogenes* within the range of 10^3 - 10^8 CFU/mL was observed. In addition, the sensor demonstrated high specificity and selectivity towards the target in the presence of other bacterial cells such as *Salmonella* Typhimurium and *Escherichia coli* O157:H7. To facilitate the demand for on-site detection, the sensor was integrated into a smartphone-controlled biosensor platform, consisting of a compact potentiostat device and a smartphone. The signals from the proposed platform were compared with a conventional potentiostat using the immunosensor interacted with *L. monocytogenes* (10^3 - 10^5 CFU/mL). The signals obtained with both instruments showed high consistency. Recovery percentages of lettuce homogenate spiked with 10^3 - 10^5 CFU/mL of *L. monocytogenes* obtained with the portable platform were 90.21, 90.44, 93.69, respectively. Therefore, the presented on-site applicable SWCNT-based immunosensor platform was shown to have high potential to be used in field settings for food and agricultural applications.

3.1. Introduction

Food safety has attracted significant attention due to continued outbreaks (King et al., 2017; Nyachuba, 2010). It was estimated that in the United States, 1 in 6 people are sickened from consumption of contaminated foods each year and 3,000 die (CDC, 2018). *Listeria monocytogenes* (*L. monocytogenes*) is one of the most dangerous foodborne pathogens which causes a fatal disease, listeriosis. Although the incidence of listeriosis is generally low, it has been reported that specific group of populations including pregnant women, newborn infants, and immunocompromised adults, have increased susceptibility to listeriosis (Silk et al., 2014; Swaminathan & Gerner-Smidt, 2007). *L. monocytogenes* is widely distributed in the environment and there has been an increasing trend in fresh produce-associated listeriosis outbreaks such as chopped celery, whole cantaloupes, lettuces, and packaged salads (Zhu, Gooneratne & Hussain, 2017).

Conventional methods for detection and identification of pathogenic microorganisms include traditional culture plating (gold standard method), polymerase chain reaction (PCR), and enzyme-linked immune-sorbent assay (ELISA) (Chen et al., 2016; Jadhav, Bhave & Palombo, 2012; Sharma & Mutharasan, 2013). Although the above methods are highly reliable, they are time-consuming and labor-intensive. In addition, these analyses require operations by well-trained personnel in laboratory settings. As a consequence, there is a real need for the development of sensitive, accurate, and rapid detection method that can be employed for on-site detection (Arora et al., 2011; Majumdar, Chakraborty & Raychaudhuri, 2013).

Biosensor-based detection method has been proposed as a promising alternative due to its simplicity, cost-efficiency, and potential field applications (Mello & Kubota, 2002). In particular, electrochemical impedance spectroscopy (EIS)-based biosensor has received much attention as it allows for a label-free detection of various analytes with high sensitivity (Bogomolova et al., 2009).

The EIS-based immunosensor analyzes changes in the electron transfer resistance (R_{et}) at a bio-interface, which arises from the antigen-antibody interaction. The R_{et} is obtained by measuring the response of an electrochemical cell to a small amplitude of sinusoidal voltage as a function of wide range of frequency (Prodromidis, 2010; Wang, Ye & Ying, 2012). The forte of this technique is its ability to measure subtle changes in the electrical properties of an electrode surface, thus elevating the sensitivity. Lu et al. (2013) presented an impedimetric *Escherichia coli* (*E. coli*) K12 biosensor with a limit of detection (LOD) of 10^3 CFU/mL using biotinylated antibodies tethered to streptavidin on a microwire electrode. Chowdhury et al. (2012) also reported EIS-based detection of *E. coli* O157:H7 using the polyaniline surface with a LOD of 10^2 CFU/mL.

Numerous nanomaterials-based biosensors have been developed for improved sensitivity and response time (Ferrier, Shaver & Hands, 2015; Rodriguez et al., 2015). Among a large variety of nanomaterials, a single-walled carbon nanotube (SWCNT) has been suggested as the most applicable nanomaterial due to its unique properties. A SWCNT offers significant advantages such as fast electron transfer capability, high surface area, and physicochemical stability (Allen, Kichambare & Star, 2007; Heller et al., 2008). Yamada et al. (2014) reported that a SWCNT-modified junction sensor enhanced the signal by seven-folds compared to the sensor without the aid of SWCNTs upon the recognition of *E. coli* cells. Chunglok et al. (2011) incorporated SWCNTs to ELISA to detect 10^3 CFU/mL of *Salmonella enterica* serovar Typhimurium (*S.* Typhimurium).

Recently, a smartphone integrated biosensing module has been developed for on-site analysis (Vashist et al., 2015; Zangheri et al., 2015). A smartphone is the most widely used mobile devices with functions such as high-speed processor, powerful CPU, and wireless communication (Zhang et al., 2015; Zhang & Liu, 2016). Within the proposed biosensing platform, the commands

of electrochemical analysis originate from the smartphone and the results are displayed in real-time (Wang et al., 2017; Zhang & Liu, 2016). Therefore, cost-effective and in-field applicable biosensing apparatus could be developed.

In this study, a SWCNTs-based immunosensor was developed and integrated into a smartphone-controlled EIS platform for the detection of *L. monocytogenes.* In this platform, the bio-molecular interactions were converted into impedance signals and transmitted wirelessly to a smartphone by a hand-held EIS transducer. An Android application was developed to control the electrochemical measuring process and the results of analysis are displayed graphically in real-time. The analytical performance of the proposed smartphone-controlled biosensor was compared with a reference laboratory potentiostat.

3.2. Materials and Methods

3.2.1. Microwire sensor fabrication

The microwire functionalization method was adapted from Yamada et al. (2014) with minor modifications. 7% gold plated tungsten wire (50 µm in diameter, ESPI Metals, Ashland, OR) was cut into 25 mm length and sanitized by sonicating in distilled water and 70% alcohol for 5 min each. The wires were then dried in a furnace at 175°C for 10 min. The sanitized microwires were mounted onto the automated XYZ stage controlled by the COSMOS program for the surface modifications (Franklin Mechanical & Control Inc., Gilroy, CA; Velmex, Inc., Bloomfield, NY). The microwire surfaces were coated with 1% polyethylenimine (PEI, branched, average Mw ~ 25,000, Product # 40827) and 0.01% single-walled carbon nanotubes (SWCNTs; SWNT PD1.5L, NanoLab, Inc., Waltham, MA) dispersed in N,N-dimethylformamide (DMF; Sigma Aldrich, St. Louis, MO) sequentially by dipping and withdrawing method at a velocity of 6 mm/min. 5 µL of streptavidin (from *Streptomyces avidinii*, Sigma Aldrich), 5 µL of biotinylated polyclonal *L. monocytogenes* antibodies (from rabbit, #PA 1-85650, Thermo Fisher Scientific, Waltham, MA), and 5% bovine serum albumin (BSA; #A3294, Sigma Aldrich) were dropped on the PEI-SWCNTs coated wires in a step-wise manner for the recognition of antigen using polydimethylsiloxane (PDMS; Sylgard 184 silicone elastomer curing agent and base, Dow Corning, Midland, MI) as a support.

3.2.2. Microbial preparation

Frozen stock cultures of *E. coli* O157:H7, *L. monocytogenes* (F2365), and *S.* Typhimurium (ATCC 14028) were obtained from the Food Microbiology Lab, University of Hawaii. All experiments were conducted in a certified biosafety level II laboratory. 100 µL of each bacterial strain was cultured separately in 10 mL of tryptic soy broth (BBL™ Trypticase ™ soy broth, BD

diagnostic systems, Franklin Lakes, NJ) and incubated for 24 h at 37°C. Each culture was serially diluted using 0.1% peptone water to obtain a range of concentrations. Microbial cocktail samples were prepared by transferring 100 µL of *L. monocytogenes* culture to 900 µL of non-target bacteria suspension. The initial concentrations of *E. coli* O157:H7, *S.* Typhimurium, *L. monocytogenes* were obtained by the plate counting method on OXOID MacConkey agar (Thermo Fisher Scientific, Waltham, MA), Xylose Lysine Desoxycholate agar (BBL™ XLD Agar Prepared Media Stacker ™Plates, BD diagnostic systems), PALCAM *Listeria* selective agar (Difco™ PALCAM Medium Base) with antimicrobic supplement, respectively. The concentrations of the individual bacterium in pure and microbial cocktail samples are summarized in Table 3.1.

Table 3.1. Concentrations of each bacteria in pure and microbial cocktail samples for specificity and selectivity test

Bacteria	Concentrations (CFU/mL)
L. monocytogenes *	1.97×10^4
E. coli O157:H7	2.63×10^4
S. Tyhimurium	1.55×10^4

*Target

Bacterial mixture	Concentrations (CFU/mL)	
	Target	Non-target
L. monocytogenes *+ *E. coli O157:H7*	2.62×10^4	1.73×10^4
L. monocytogenes *+ *S.* Tyhimurium	1.92×10^4	1.83×10^4

*Target

3.2.3. The smartphone-controlled biosensor system

The proposed smartphone-controlled biosensor system is comprised of three parts: a functionalized microwire sensor, a compact ABE-Stat potentiostat (DIAGENETIX, Inc, Honolulu, HI), and a smartphone (Figure 3.1).

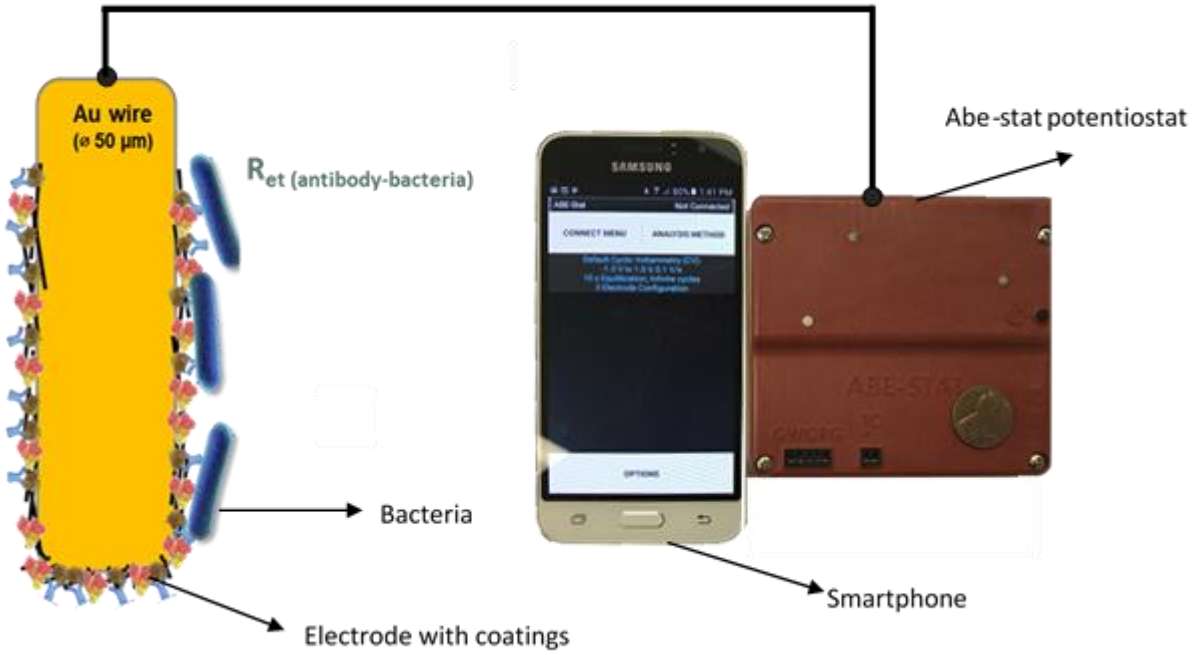

Figure 3.1. A schematic of smartphone-controlled biosensor platform. A compact potentiostat is interfaced wirelessly to a smartphone.

The potentiostat device is fully wireless-enabled by integrating Bluetooth and Wi-fi modules. The commands for EIS analysis originated from an Android app which interfaced the smartphone with the otentiostat. A reference laboratory potentiostat (µ-Autolab type III potentiostatic frequency response analyzer (FRA) equipped with NOVA software version 1.6, Metrohm Autolab USA Inc., Riverview, FL) was used to compare the performance of the

smartphone-controlled potentiostat. The EIS analysis was performed with both systems under the same conditions and parameters.

3.2.4. Detection of *L. monocytogenes*

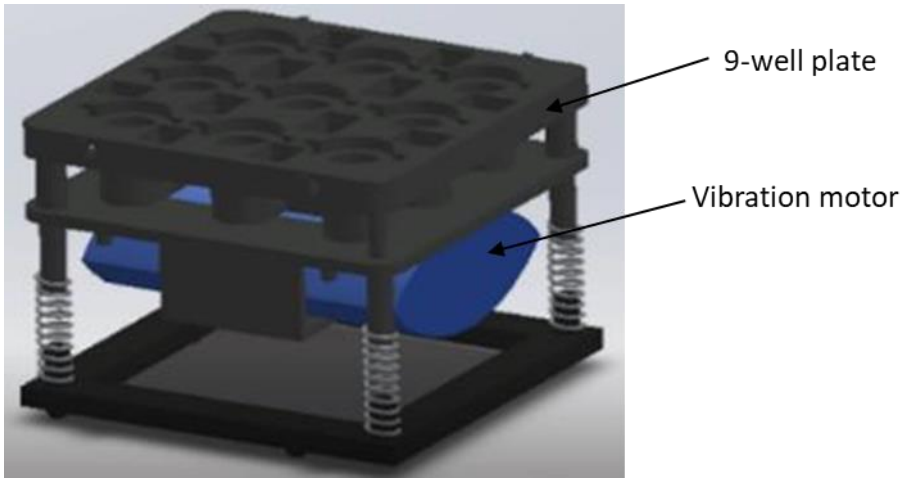

Figure 3.2. A schematic of a 9-well plate equipped with a vibration motor.

A 9-well plate was designed by a SolidWorks software (Dassaults System Solidworks Corp., Waltham, MA) and printed with a 3D printer (Form 2, Formlabs, Somerville, MA) using a standard resin (Figure 3.2). In order to enhance the recognition of the target, the designed 9-well plate was equipped with a vibration motor (Gear Motor, Uxcell, Hong Kong). 500 µL of the bacterial sample was placed in each well and the functionalized microwire was inserted to the well for 5 min to permit antibody-antigen interaction. Applying slight agitation aided in enhancing the sensitivity of the sensor by 1-log for the detection of *E. coli* K12 (data not shown). Therefore, constant agitation was applied to the plate to enhance the bioaffinity reaction. Sensitivity testing was conducted to determine the LOD of the functionalized microwire. Serial dilutions of *L. monocytogenes* were prepared from the stock culture and tested with the microwire. The specificity of the fabricated biosensor towards the target was demonstrated with pure cultures of *S.*

Typhimurium and *E. coli* O157:H7 at a concentration of 10^4 CFU/mL. The selectivity of the biosensor was examined by reacting it with the microbial cocktail solutions.

3.2.5. Preparation of lettuce homogenate

Lettuce was purchased from a local grocery store in Honolulu, Hawaii. 10 g of lettuce was homogenized with 90 mL of sterilized PBS using a stomacher (Stomacher 400 Circulator; Seward Inc., Bohemia, NY) at 260 rpm for 10 min (Mao et al., 2016). The lettuce homogenate was spiked with *L. monocytogenes* to achieve final concentrations ranging from 10^3 - 10^5 CFU/mL. The number of viable cells was plate counted on the PALCAM *Listeria* selective agar.

3.2.6. Impedance measurement

The electrochemical cell was constructed with a conventional three-electrode configuration in an electrolyte solution containing 5 mM $K_3Fe(CN)_6$, 5 mM $K_4Fe(CN)_6$, and 0.1 M KCl (product #244023, #P3289, and #P9541, Sigma-Aldrich Co., Saint Louis, MO). The functionalized microwire was used as a working electrode (WE), a platinum electrode (product #CHI 115, CH Instruments, Inc., Austin, TX) with a diameter of 0.5 mm was used as a counter electrode, and a saturated Ag/AgCl electrode (catalog #A57194, VWR International, Brisbane, CA) served as a reference electrode. The electrochemical impedance measurements were carried out within a frequency range of 0.1 Hz - 100 kHz at a DC bias potential of 200 mV and peak AC amplitude value of 10 mV. The experimental data were displayed by the Nyquist plots. The Nyquist plots obtained from the reference laboratory device were analyzed by the built-in tool in the NOVA software and the R_{et} was obtained from the equivalent circuit model as Figure 2.2 (c). The Nyquist plots from ABE-Stat were analyzed by Matlab software (Mathworks, Natick, MA) using the same

equivalent circuit model. The changes of electron transfer resistance (ΔR_{et}) at the sensor interface due to the attachment of bacterial cells at the electrode-film interface were calculated as follows:

$$\Delta R_{et} = R_{et}\,(\text{antibody-bacteria}) - R_{et}\,(\text{antibody}) \quad (3.1)$$

3.2.7. Data analysis

Three replications were performed for each experiment (n=3). The electrochemical impedance signals were averaged and standard deviations were expressed as error bars in the graphs. Statistical analysis between the means was conducted based on Duncan's multiple range tests using a single factor analysis of variance (ANOVA) in Statistical Analysis Software at 95% confidence level (SPSS Inc., Chicago, IL). The statistical analysis of the average of the electrochemical impedance measured by the portable and reference devices were conducted by independent sample t-test 95% confidence level.

3.3. Results and discussion

3.3.1. Monitoring the surface functionalization of the anti-*L. monocytogenes* immunosensor

The step-wise surface modification process was characterized by the EIS measurements in the presence of the redox couple $[Fe(CN)_6^{4-/3-}]$ (Figure 3.3). The SWCNTs adsorbed onto the surface of Au/PEI layer due to the amine-nanotube interaction. Amine groups of PEI have a high binding affinity for SWCNTs, forming polymer-SWCNT films (Rouse et al., 2004). The PEI-SWCNTs modified surface is able to bind with the negatively charged streptavidin via electrostatic and hydrophobic interactions (Lu et al., 2013; Yamada et al., 2014). Streptavidin on the modified

surface links with the biotinylated antibodies with the well-known streptavidin-biotin interaction (Darst et al., 1991).

The average R_{et} of a bare microwire was 0.317 kΩ. When the bare microwire was coated with PEI, the R_{et} increased to 2.99 kΩ, followed by a significant decrease to 0.68 kΩ when SWCNTs were introduced to the surface. The dramatic decrease in the R_{et} demonstrated that the SWCNT layer enhanced the conductivity of the electrode/electrolyte interface. Further adsorption of streptavidin, antibody, and BSA on the Au/PEI/SWCNT modified microwire increased the R_{et} to 1.85, 2.97, and 3.21 kΩ, respectively. On the electrode, the electron transfer between the redox probe $[Fe(CN)_6]^{4-/3-}$ and the electrode occurs by tunneling of electrons through the coating layers or through the unblocked sites on the surface. Hence, the surface passivation influences the R_{et} at the electrode/electrolyte solution interface.

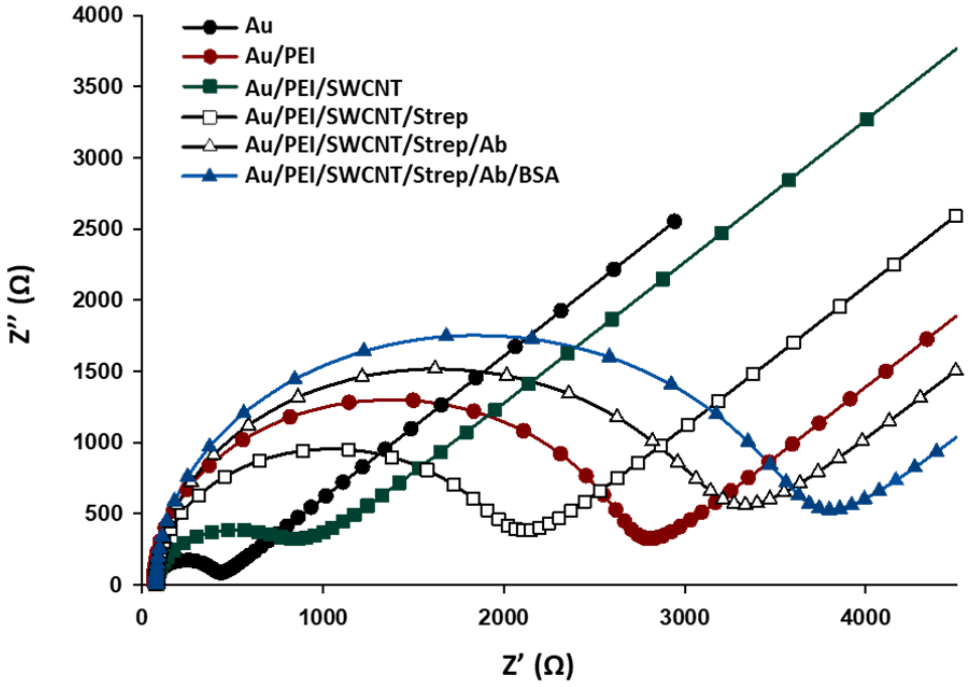

Figure 3.3. Impedance spectra of the electrode corresponding to step-wise modifications.

The observed increase in R_{et} implies that the microwire is successfully functionalized and the surface coatings hinder the charge transfer of the $[Fe(CN)_6^{4-/3-}]$ redox couple to the surface of the electrode (Liu et al., 2011). These trends are consistent with other studies as well (Bourigua et al., 2010; Chen et al., 2012). The effect of SWCNTs on the signal enhancement was evaluated as well. Figure 3.4 demonstrates that ΔR_{et} of 4.02 kΩ was observed when the SWCNTs integrated sensor was exposed to 10^7 CFU/mL *L. monocytogenes* solution. However, ΔR_{et} of 0.90 kΩ was measured with the sensor without SWCNTs when interacted with the same *L. monocytogenes* concentration. The increase in ΔR_{et} may be attributed to the elevated surface area by SWCNTs, which serves as an active binding site of the antibodies.

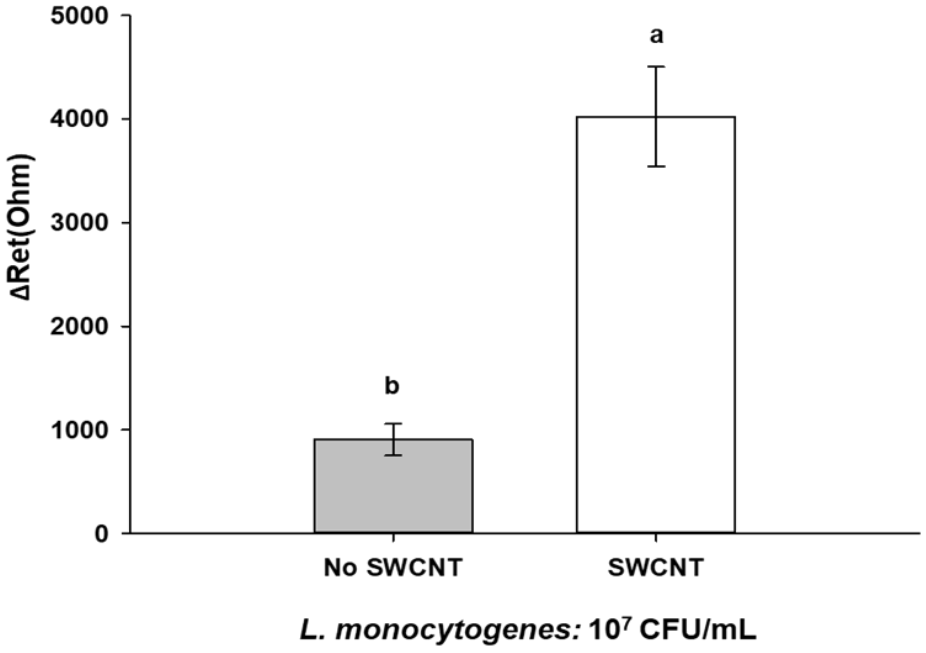

Figure 3.4. Change in the electron transfer resistance in response to *L. monocytogenes* captured on the sensor with and without SWCNTs. Significant difference between signal measurements are indicated by the different superscripts at a 95% confidence level .

3.3.2. Performance of the *L. monocytogenes* biosensor

The sensors were exposed to stepwise increasing concentrations of *L. monocytogenes* and microbial cocktail solutions to assess the performance of the sensor (sensitivity, selectivity, and specificity) before deployed in a real food sample. These were evaluated with the conventional laboratory instrument. The sensitivy of the sensor was evaluated with serially diluted *L. monocytogenes* cultures. A linear relationship was obtained in the range of 10^3 - 10^8 CFU/mL (R^2 = 0.982) with a LOD of 1.4×10^3 CFU/mL (Figure 3.5) Each data point represented a mean value obtained from three independent microwire sensors; error bars represented the standard deviation of the three measurements. As expected, a greater ΔR_{et} was measured as the bacterial concentrations in the samples increased, i.e. increased electron transfer resistance of a redox probe of $Fe(CN)_6^{3-/4-}$ at the electrode/electrolyte interface. This change in the electrical properties of the sensor could be attributed to the highly insulating properties of the cell membrane. It was found that the conductivity of the cell membrane is significantly lower (approximately 10^{-7} S/m) than the interior of a cell (1 S/m) (Jain et al., 2012). As a result, the attachment of the bacterial cells retards the interfacial electron-transfer kinetics and thus increases the R_{et}.

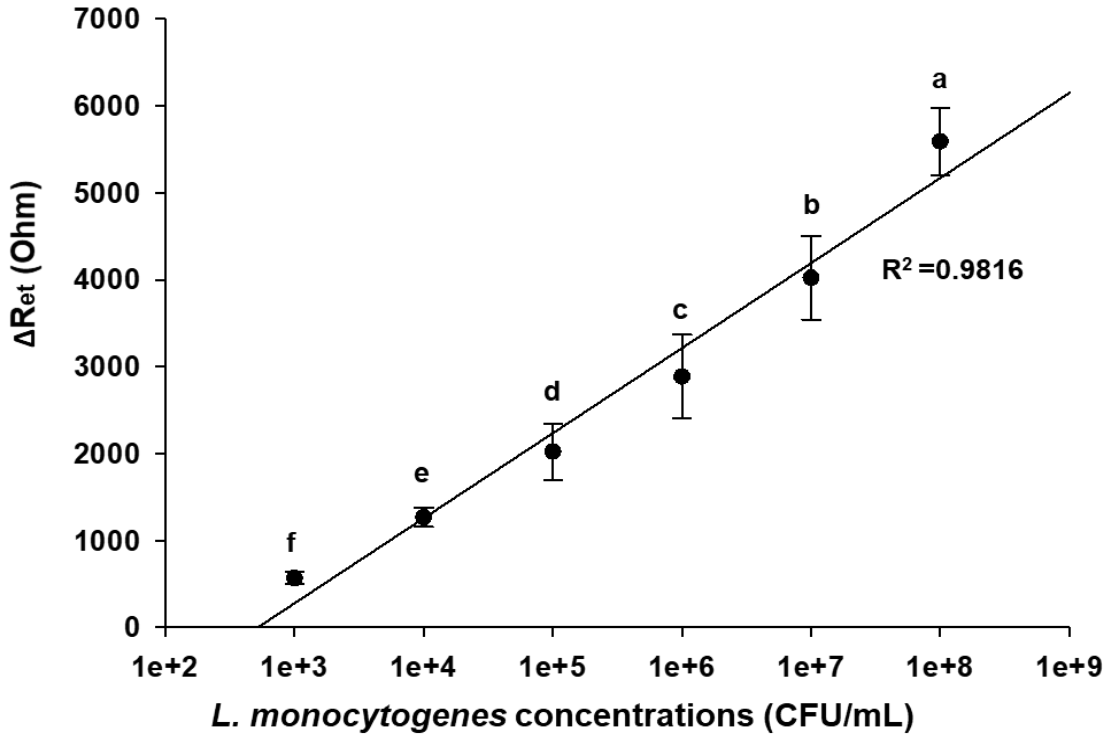

Figure 3.5. Relationship between changes in the electron transfer resistance and concentrations of *L. monocytogenes* (10^3 - 10^8 CFU/mL) bound to the sensor. Significant differences between signal measurements and bacteria concentration are indicated by the different superscripts at a 95% confidence level.

Specificity is a crucial factor in developing a microorganism detection tool. The specificity of the anti-*L. monocytogenes* sensor was evaluated by comparing the signals against pure *L. monocytogenes* (10^4 CFU/mL) to pure *E. coli* O157:H7 and *S.* Typhimurium cultures (10^4 CFU/mL), individually. Data represented in Figure 3.6 indicate that the sensor's response to pure culture of *E. coli* O157:H7 and *S.* Typhimurium resulted in the ΔR_{et} of 185 and 220 Ω, respectively. This may be partly due to the non-specific binding at the surface of the electrode. However, when the sensor was exposed to pure suspension of *L. monocytogenes* (10^4 CFU/mL), a significant increase in the ΔR_{et} was observed. This recognition is achieved by the induced immune complex

reaction on the surface of the sensor. These results indicate that the anti-*L. monocytogenes* sensor exhibits negligible responses to the non-targets, demonstrating high specificity to the target over the other bacteria.

The selectivity of the biosensor was studied to evaluate the possible interference on the sensing signals. The selectivity of the proposed sensor towards *L. monocytogenes* was evaluated by challenging it with microbial mixture samples (*L. monocytogenes* and *E. coli* O157:H7, and *L. monocytogenes* and *S.* Typhimurium at 10^4 CFU/mL concentrations). When the sensor interacted with mixtures of EC + LM and ST + LM, the obtained ΔR_{et} values were 1025 ± 35 and 1260 ± 198 Ω, respectively. These signals were close to the sensor's response when it was introduced to 10^4 CFU/mL of pure *L. monocytogenes*, 1205 ± 350 Ω. These results demonstrate that the electron transfer behavior remained unchanged with the presence of non-target bacteria such as *E. coli* O157:H7 and *S.* Typhimurium. These findings were considered to originate from the antibody-antigen reactions as well as the saturation of the unoccupied sites with BSA. The variable regions on the heavy chains and light chains on the antibody and the epitopes on the antigen ensure the specificity of the sensor analysis (Killard et al., 1995). In addition, BSA serves as a blocking agent for its capability of saturating the unoccupied sites without participating in the immunochemical reactions in the assay (Jeyachandran et al., 2009).

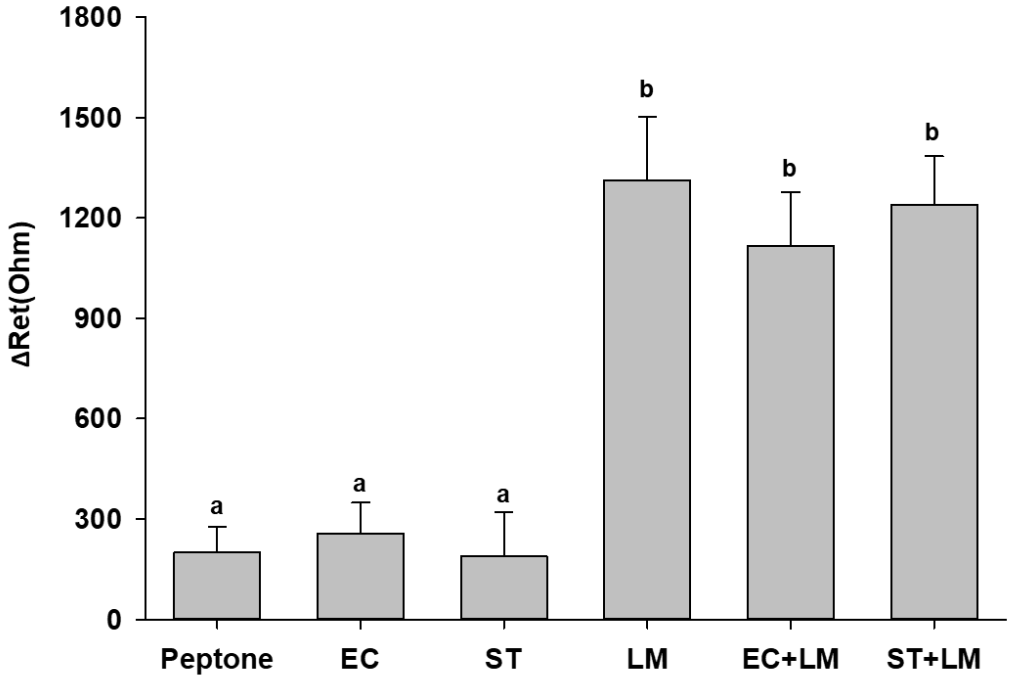

Figure 3.6. Specificity and selectivity testing of *L. monocytogenes* sensor. Acronyms represent pure bacteria suspension and bacterial mixtures; EC: *E. coli* O157:H7, ST: *S.* Typhimurium, LM: *L. monocytogenes*, EC + LM: a mixture of *E. coli* O157:H7 and *L. monocytogenes*, ST + LM: a mixture of *S.* Typhimurium and *L. monocytogenes.*

3.3.3. Performance of the smartphone-controlled platform for *L. monocytogenes* detection

The applicability of the proposed smartphone-controlled system was demonstrated by analyzing R_{et} of the functionalized sensors and immunologically interacted sensors with comparison to the reference laboratory instrument. As shown in Figure 3.7, the portable platform was able to detect the same range of concentrations of the target (10^3 - 10^5 CFU/mL) as the reference instrument. The control represents the R_{et} of the sensors with coatings and thus, may have resulted in small variation. Additionally, although slight variations were apparent, the obtained R_{et} values were statistically comparable with the reference device. The slight variations

in the values between the two systems could be partially attributed to the non-linear nature of redox processes and discontinuities at several characteristic frequencies (Jenkins et al., 2019).

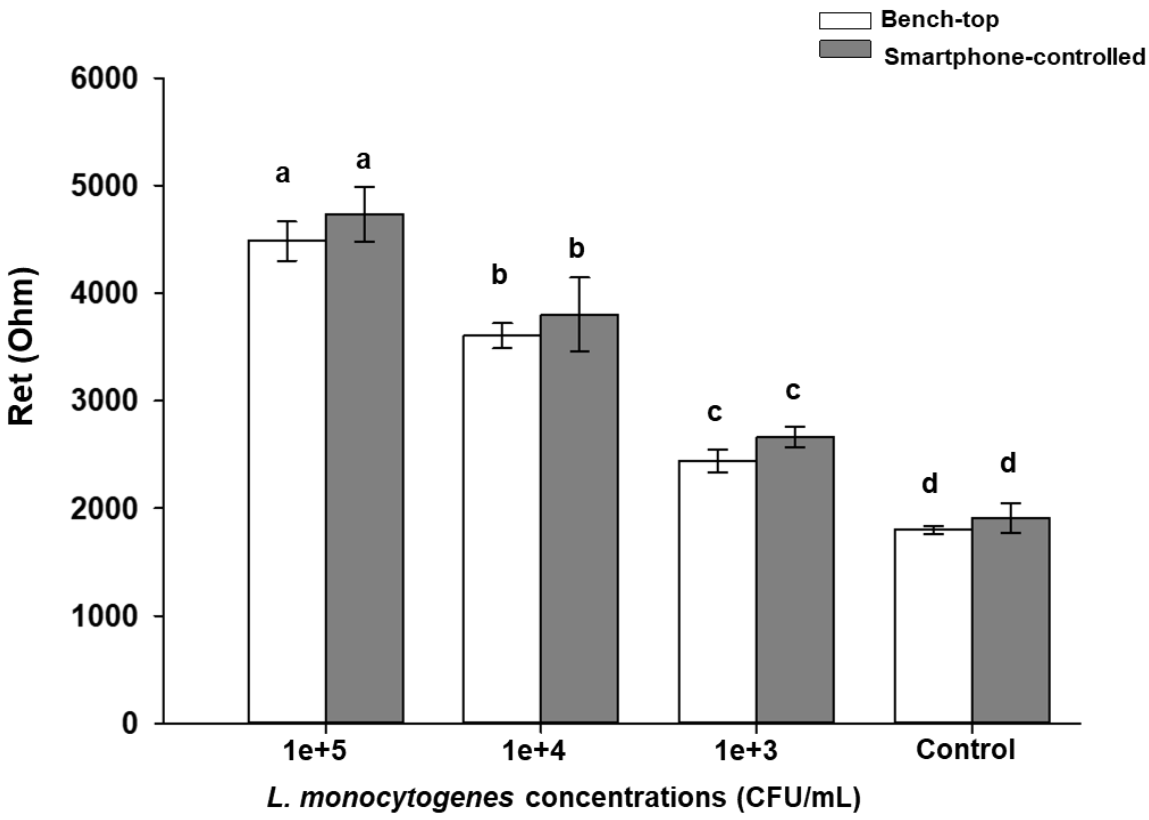

Figure 3.7. Electron transfer resistance obtained by the bench-top and smartphone-controlled system in response to 10^3 - 10^5 CFU/mL of *L. monocytogenes*. Significant differences between concentrations are indicated by different superscripts at a 95% confidence level.

A similar trend was observed in the study of Jenkins et al. (2019), in which the electrochemical impedance spectroscopy scanning of the bare and coated 50 µm gold-plated tungsten wires with both ABE-Stat and the reference laboratory device resulted in reasonably close data; however, slight deviations were present. Although unable to fully explain this phenomenon, the network analyzer chip used in the ABE-Stat may have resulted in variations and distortions at a certain frequency range when conducting the analyses (Jenkins et al., 2019). Despite the

discrepancies, the presented platform significantly reduced the overall size and the cost of the platform compared to the reference laboratory potentiostat. The total cost of the ABE-Stat ranges from US$152.50-US$215 depending on the quantity manufactured (Jenkins et al., 2019). This price is approximately 1% of the reference laboratory instrument. In terms of weight, the ABE-Stat potentiostat weighed only 2.7% of the reference laboratory device (4.99 kg).

3.3.4. Detection of *L. monocytogenes* in the lettuce homogenate

The accuracy of the proposed smartphone-controlled platform for the detection of *L. monocytogenes* in food samples was assessed by the recovery experiments. Prior to detecting the target bacterial cell, the influence of lettuce homogenate on the sensing signal was evaluated. The sensor was exposed to both target-free lettuce homogenate and sterilized peptone water (reference blank solution) and the ΔR_{et} values were compared. The results showed that the anti-*L. monocytogenes* sensor's responses to lettuce homogenate were not significantly different to the

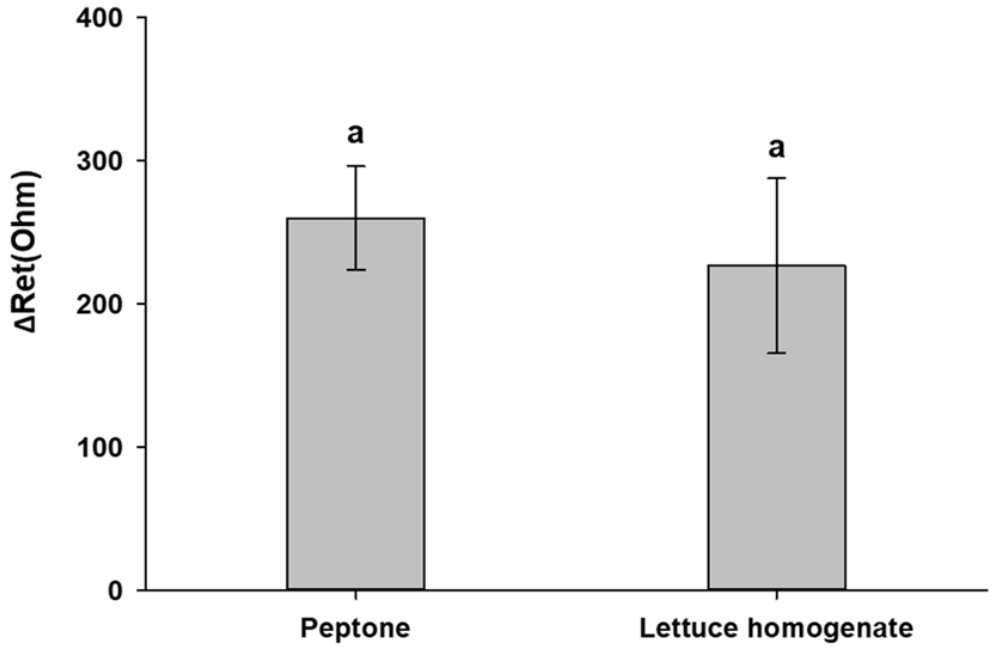

Figure 3.8. Effect of lettuce homogenate on the ΔR_{et} of the sensor.

blank buffer solution (Figure 3.8). This implies that lettuce homogenate did not alter the sensing signal of the sensor.

Based on the previous findings, lettuce homogenate was spiked with 10^3 - 10^5 CFU/mL of *L. monocytogenes* and the ΔR_{et} was evaluated with both the reference device and smartphone-controlled platform. The recovery rate of the bacteria from lettuce homogenate was obtained according to the calibration curve. As shown in Table 3.2, the recovery percentage ranged from 88.48% to 95.38% for the bench-top and 90.21% to 93.69% for the proposed portable device. These high recovery rates indicate that the proposed platform was applicable for the detection of *L. monocytogenes* in food samples.

Table 3.2 Recoveries of *L. monocytogenes* in lettuce homogenate using the proposed method

Sample	Original value (CFU/mL)	Spiked concentration (CFU/mL)	Detected (CFU/mL)		Recovery (%)	
			Bench-top	Smartphone	Bench-top	Smartphone
1	0	1.29×10^3	1.1414×10^3	1.1637×10^3	88.48	90.21
2	0	1.04×10^4	9.920×10^3	9.406×10^3	95.38	90.44
3	0	1.15×10^5	1.0465×10^5	1.0774×10^5	91.05	93.69

3.4. Conclusion

In this study, a SWCNT-based electrochemical immunosensor for on-site detection of *L. monocytogenes* was developed. The limit of detection of the sensor was 10^3 CFU/mL with a detection time of 10 min. In addition, the sensor demonstrated high specificity and selectivity towards the target. In order to facilitate the requirements for on-site screening for food safety, the sensor was integrated into a smartphone-controlled platform. The performance of the proposed system was comparable to the reference instrument and exhibited high applicability for analyzing food samples. In the future, bacterial cell concentration methods such as dielectrophoresis and immunomagnetic separation can be combined to further improve the sensitivity of the sensor.

Chapter 4.

A NANOPOROUS STAINLESS STEEL SURFACE TO PREVENT ADHESION OF *LISTERIA MONOCYTOGENES* FOR IMPROVED FOOD SAFETY

Abstract

Bacterial attachment on food-contact surfaces and subsequent biofilm formation is a significant problem in the food industry. Bacterial cells dispersed from biofilms are a major source of contamination and a cause of equipment failure. Superhydrophobic (SH) surface (water contact angle (WCA) > 150°) modification has potential to prevent bacterial adhesion by minimizing the contact area between the bacterial cell and the surface. In this study, a stainless steel-based SH surface was fabricated by manipulating nanostructures via electrochemical etching and polytetrafluoroethylene (PTFE) film. The formation of nanostructures on the stainless steel surfaces were characterized by field emission scanning electron microscopy (FESEM). The substrates etched at 10 V for 5 min and 10 V for 10 min with PTFE deposition resulted in an average WCAs of 154° ± 4° with pore diameter of 50 nm. In addition, the adhesion of *Listeria monocytogenes* was decreased up to 99% on SH surfaces compared to the bare substrate. The biofilm resistance characteristics of the SH surface (10 V 5 min with PTFE) was evaluated with a CDC biofilm reactor as well. On the SH surface, the bacterial biofilm population was reduced by 1.8 log CFU/mL compared to the control surface. These findings demonstrate the potential for the development of anti-bacterial and anti-biofilm surfaces via incorporating nanoporous patterns with PTFE films.

4.1. Introduction

Bacterial adhesion on food-contact surfaces and subsequent biofilm formation has been recognized as a serious public health threat (Evans et al., 1998). Biofilms are an assemblage of surface-associated microbial cells enclosed in self-produced extracellular polymeric substance (EPS). Biofilm refers to not only the bacterial cells but also noncellular materials trapped within the EPS such as mineral crystals, corrosion particles, and silt particles (Donlan, 2002; Hood & Zottola, 1995). In general, the mechanisms of bacterial adhesion on a substratum are categorized into two processes: a two-step process and a three-step process (Hood & Zottola, 1995; Mittelman, 1998). The two-step process involves reversible and irreversible adhesion steps. In the reversible step, bacteria can be easily removed by the application of a mild shear force and involves van der Waals and electrostatic forces. Once adsorbed, the irreversible step initiates and produces the EPS. Several short-range forces such as dipole-dipole interaction, hydrogen bonds, and ionic covalent bonding are involved in the irreversible step (Mittelman, 1998). The three-step process views bacterial adhesion in terms of the distance between the bacteria and the surface (Hood & Zottola, 1995). At separation distances > 50 nm, the adhesion is reversible and long-range forces such as electrostatic and van der Waals forces operate. At the distance about 20 nm, the attachment involves long-range forces as well as electrostatic interactions and the reversible adhesion becomes irreversible over time. The last step occurs at the distance < 15 nm and produces adhesive polymers, resulting in irreversible attachment (Hood & Zottola, 1995).

It is difficult to eradicate biofilms from the food processing plant as the produced EPS protects the enclosed cells against harsh environmental conditions such as shear stress, biocides, and disinfectants (Flemming, 1993). In addition, the detachment of microorganisms from biofilms may contribute to food spoilage, cross-contamination, and spread of foodborne pathogens (Van

Houdt and Michiels, 2010; Zottola and Sasahara, 1994). Therefore, the extensive research has been conducted to prevent biofilm-related surface contamination including antibiotic releasing surfaces and anti-bacterial coated surfaces (Knetsch and Koole, 2011; Qian et al., 2002; Tiller et al., 2001; Yu et al., 2015). However, drawbacks such as practical applications, costs, and increased bacterial resistance continue to remain.

Recently, a superhydrophobic (SH) surface has been proposed as a potential anti-bacterial surface. The SH surfaces are characterized by high water contact angle ((WCA) $> 150^{o}$)) with self-cleaning and anti-corrosion properties (Bruzaud et al., 2017; Gu et al., 2017; Jeevahan et al., 2018; Mohamed et al., 2015). These surfaces resist bacterial colonization by reducing the adhesion force between the bacteria and a solid surface. Superhydrophobicity can be induced on a surface by introducing micro/nano hierarchical structures and a low surface energy material. Polytetrafluoroethylene (PTFE) is an artificial fluoropolymer with an exceptional hydrophobicity and a low surface energy (20 mN/m at 20°C) (Yasuda et al., 1994). Pure PTFE coating on a flat surface does not promote superhydrophobicity as the WCA of PTFE is around 120°; however, introducing nanoporous structures by electrochemical etching in tandem with PTFE coating is expected to amplify the hydrophobicity.

Listeria monocytogenes (L. monocytogenes) is a major foodborne pathogen, which can attach to food-contact surfaces and form biofilms. This bacterium causes listeriosis in the immunocompromised individuals including pregnant women and has a high mortality rate (Rocourt et al., 2000). Therefore, the aims of this study were to fabricate a SH substrate by electrochemical etching and PTFE coating and to demonstrate the anti-bacterial and anti-biofilm activities against *L. monocytogenes*.

4.2. Materials and Methods

4.2.1. Fabrication of nanoporous stainless steel surface

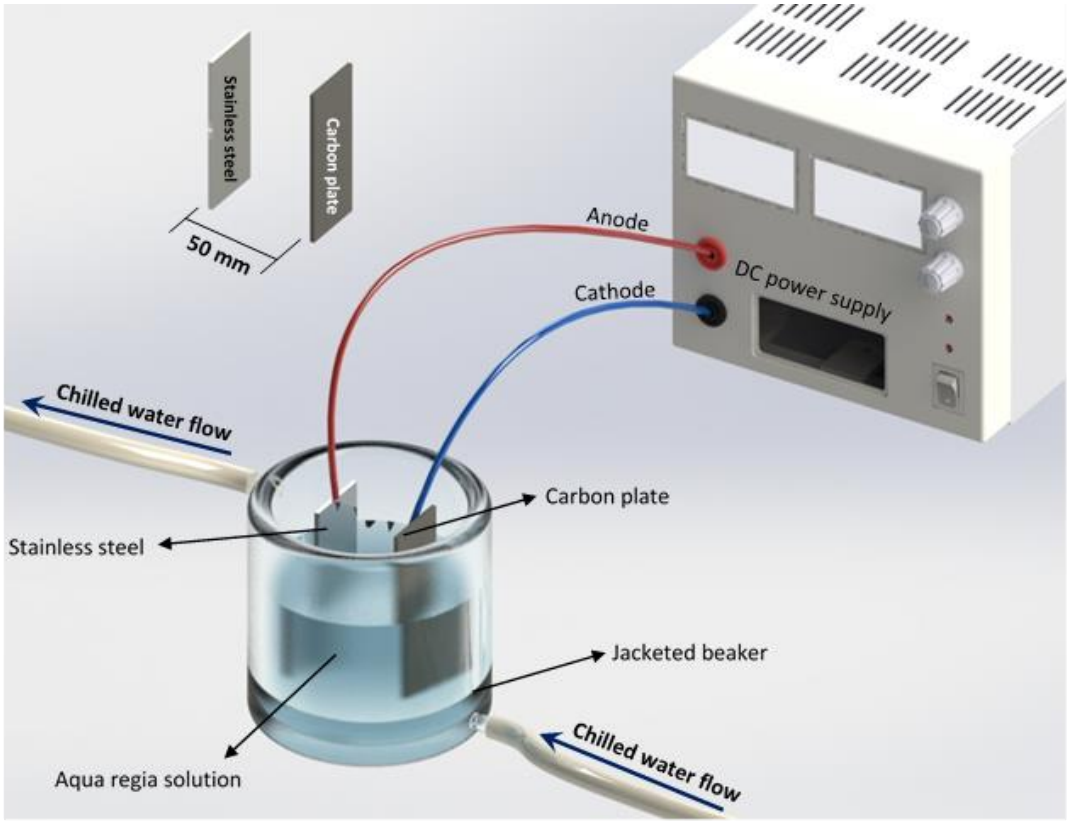

Figure 4.1. A schematic of electrochemical etching set-up.

Stainless steel 304 were cut into 25 × 20 × 0.2 mm specimen and degreased in ethanol and distilled water for 10 min using a sonication. The cleaned and dried specimen was placed in a jacketed beaker containing 200 mL of 1:1 ratio (v/v) of dilute aqua regia solution (3.6% HCl and 1.2% HNO_3) at 4°C for dissolution (Figure 4.1). Constant electric potentials of 5, 10, and 15 V were applied for 5, 10, and 15 min by a DC power supply (CPX400SP; AIM TTi, Hungtingdon, Cambs) to manipulate the pore sizes. The stainless steel served as a working electrode (anode) and the carbon plate was used as a counter electrode (cathode). This method was adapted from Lee et al. (2015) with minor modifications. PTFE solution was prepared by dissolving 0.2% w/w of

Teflon AF1600 powder (Sigma-Aldrich, St. Louis, MO) in perfluoro-compounds FC-40 (Sigma-Aldrich, St. Louis, MO) and pipetted on the electrochemically etched coupons. The coupons were baked on a hot plate at 110°C for 10 min, at 165°C for 5 min, and at 330°C for 15 min sequentially. The surface modified coupons were rinsed with distilled water for 5 min and completely dried. 5 μL of a sessile water droplet was dropped on each specimen to measure the WCA. The WCA was measured with FTA-1000 contact angle goniometer (First Ten Ångstrom, Portsmouth, VA). A flow chart of the SH fabrication process is shown in Figure 4.2.

4.2.2. Bacterial strains and culture preparation

L. monocytogenes (F2365) was provided from the Food Microbiology Laboratory (University of Hawaii at Manoa, Honolulu, HI). 100 μL of the isolate was cultured in 10 mL of tryptic soy broth at 37°C for 24 h to make a stock culture. After the incubation, the cells were centrifuged at 4,000 × *g* for 20 min and washed three times with 100 mM phosphate-buffered saline (PBS) at pH 7.1 - 7.4. The resulting pellets were resuspended in 10 mL of sterilized PBS.

4.2.3. Bacterial adhesion and biofilm formation

The bacterial attachment experiment was performed by adhering 60 μL of *L. monocytogenes* (10^9 CFU/mL) on the specimens. The specimens were stored at room temperature for 24 h and the number of attached bacterial cells was quantified. The biofilms were grown with a CDC biofilm reactor (Biosurface Technologies Corp., Bozeman, MT) and the method was adapted from Jimenez-Ruiz et al. (2015). The reactor consisted of 1-liter glass vessel which provided 350 mL of operational fluid capacity. A polyethylene top supported eight independent coupons, a medium-inlet port, and a gas-exchange port. The vessel was equipped with a baffled magnetic stir bar to provide a constant flow of 80 rpm in conjunction with a stir plate. The reactor

was filled with 350 mL of sterilized 1:20 TSB and 3.5 mL of *L. monocytogenes* culture was inoculated into the vessel. The CDC biofilm reactor was operated in a batch mode for the first 24 h at room temperature. Following the initial 24 h incubation, a continuous flow of the medium was flushed through the reactor at a flow rate of 0.77 mL/min for another 24 h.

4.2.4. Bacterial enumeration

Following the bacterial adhesion and biofilm formation experiments, the number of bacterial populations on the coupon was quantified. The coupon was placed in a test tube containing 10 mL of sterile PBS with 2 g of glass beads. The test tubes were vortexed for 2 min to dislodge the attached cells. The cell suspension was tenfold serially diluted in 0.1% peptone water and enumerated by plating serial dilutions onto PALCAM *Listeria* selective agar (Difco™ PALCAM Medium Base) with antimicrobic supplement for enumeration.

4.2.5. FESEM analysis

A FESEM equipment (Hitachi S-4800, Pacific Biosciences Research Center, University of Hawaii) was used to visualize the surface topography.

To visualize the bacterial adhesion, the specimens were submerged in 2.5% glutaraldehyde in 0.1 M cacodylate buffer twice for 10 min each. For post-fixation, specimens were submerged in a mixture of 1% osmium tetroxide and 0.1 M cacodylate buffer for 30 min. The bacterial cells were dehydrated with graded ethanol series of 10, 20, 30, 50, 70, 85, and 95%, and 100% for 10 min each and coated with a gold/palladium layer. The specimens were positioned in a critical point drier filled with liquid carbon dioxide and softly dehydrated by evaporating liquid carbon dioxide. The coupons were mounted onto aluminum stubs using carbon tape and coated with a thin gold/palladium layer using a Hummer 6.2 sputter coater for 45 seconds. Biofilm structures on

stainless steel were observed by following the same ethanol dehydration procedure and soaking it in 25%, 50%, 75%, and 100% HDMS for 10 min. After soaking in HDMS, the samples were dried by air drying and coated with a thin gold/palladium following the same procedure as above.

4.2.6. Statistical analysis

Three replications were performed for the fabrication of the superhydrophobic surfaces and the microbial analysis. Statistical analysis between the means were conducted using ANOVA based on Duncan's multiple range test with a confidence level of 95% using SPSS (ver. 20, IBM, Armonk, N.Y.).

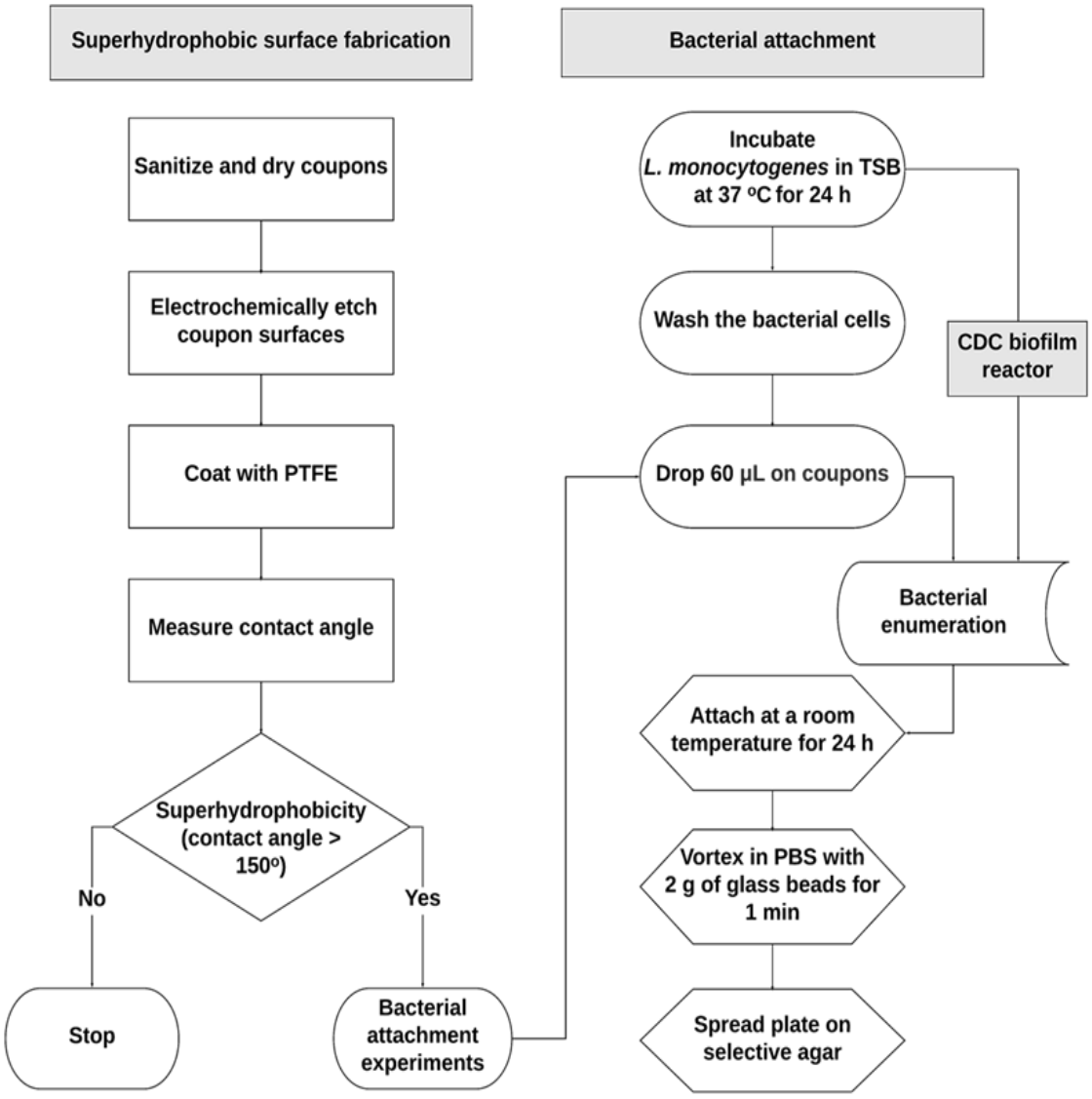

Figure 4.2. A flow chart of superhydrophobic surface fabrication and microbial experiment process by different superscripts at a 95% confidence level.

4.3. Results and Discussion

4.3.1. Effect of treatments on water contact angles of stainless steel

Figure 4.3 shows that the bare substrate exhibited WCAs below 90°. On the other hand, all the electrochemically etched surfaces resulted in WCAs greater than 90°. This implies that the increased hydrophobicity was attributed to the formation of the nanopores. These pores form air pockets between the solid/water interface and prevent water from completely touching the surface (Bormashenko et al., 2006). Within the electrochemically etched surfaces, different wetting behaviors could be observed with respect to various treatment parameters such as voltage and time. A previous study reported that the electrochemical etching parameters determined the surface micro/nanostructures, which is associated with the surface hydrophobicity (Jang et al., 2017). The WCAs of the surfaces electrochemically etched at a potential of 5 V for different treatment times were not significantly different. This finding might be caused by a small current flow through the electrochemical circuit linked to the low applied potential, which could result in the insufficient dissolution of the bare surface characteristics (Choi et al., 2016).

The average WCAs of the surfaces exhibited the highest elevation to 130° ± 3.3° and the values were not statistically different when abraded at these conditions: 10 V for 5, 10, 15 min, and 15 V for 5 and 10 min. These results demonstrated that transforming the bare to nanostructured surfaces could significantly increase the surface hydrophobicity. However, it was not sufficient to obtain a SH surface (WCA > 150°). Therefore, the above etching conditions were chosen for further investigation in enhancing the hydrophobicity with a low surface energy material, i.e. PTFE. When PTFE was deposited on the bare surface, the WCA increased from 86° to 117°. This indicated that nanostructures incorporated with PTFE film is needed to reach the superhydrophobic characteristic as well. According to Figure 4.3, SH substrates were achieved by adhering PTFE

films on the surfaces electrochemically etched at the following conditions: 10 V for 5 and 10 min (shown in red). The average surface hydrophobicity increased substantially by 79% on these SH surfaces compared to the bare substrate.

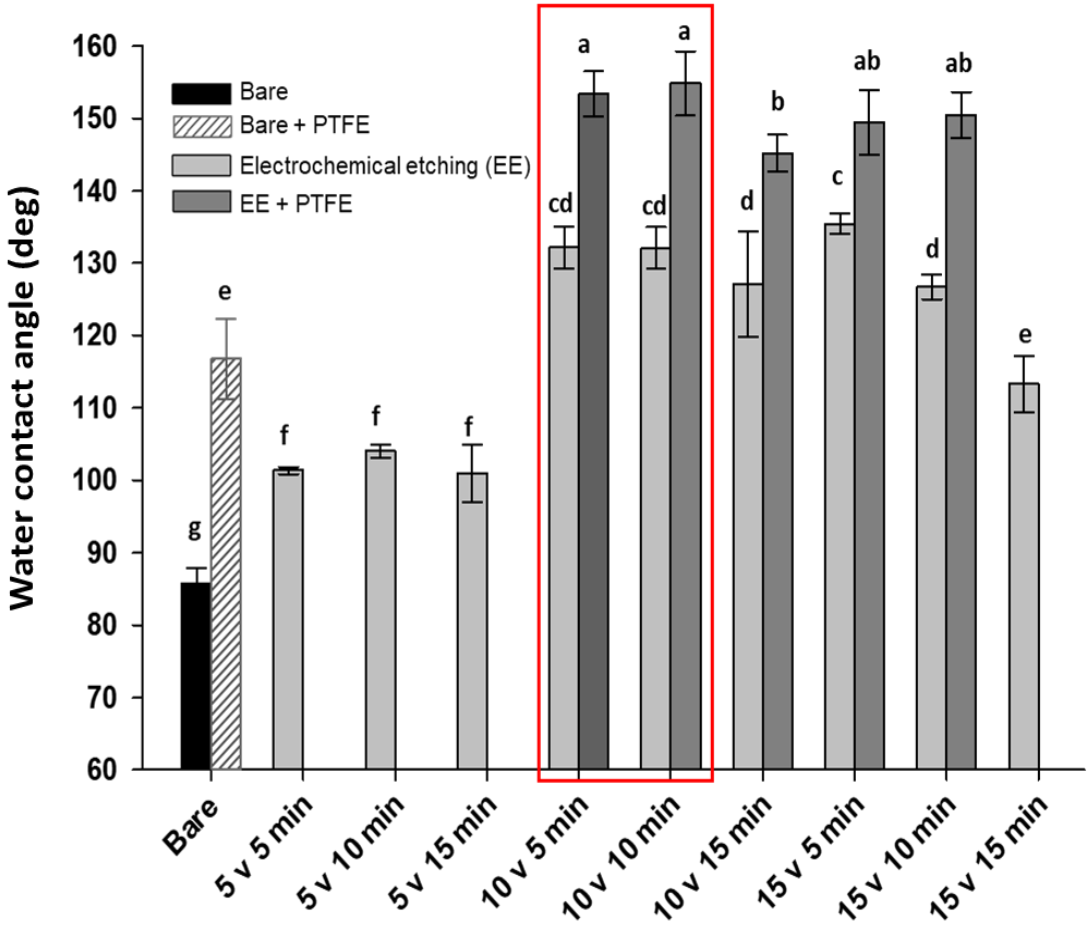

Figure 4.3. Water contact angles on surfaces modified under different etching conditions. Significant differences between etching conditions are indicated by different superscripts at a 95% confidence level.

Based on the statistical analysis from Figure 4.3, the surface morphology of the stainless steel etched at different parameters were investigated with SEM images. Figure 4.4 shows SEM images of the as-received and electrochemically etched surfaces. The as-received surface clearly displayed the typical deep-trench crevices and defects from the manufacturing process (Figure 4.4 (a)). When a potential of 5 V was applied, it resulted in incomplete removal of the initial features, i.e. crevices as well as nanopore formation due to the low material dissolution. Based on Figure 4.4 (b), the substrate with the highest increase in WCA (10 V 10 min) possessed nanopores with an average diameter of 50 nm. On the other hand, the substrate etched at 15 V for 10 min resulted in an average nanopore diameter of 70 nm with few pits (Figure 4.4 (c)). Li et al. (1998) and Choi et al. (2016) reported that the increased applied voltage resulted in a higher current flow between the electrodes, leading to cracks with disordered pores. Therefore, this could be one of the reasons the hydrophobic properties were slightly lower on the surfaces etched at 15 V compared to 10 V. According to Figure 4.4 (d) and Figure 4.4 (e), the nanoporous surface etched at the same potential (15 V) for different treatment times exhibited different pore diameters. The surface etched for the extended time (15 min) clearly displayed pits with bigger pore diameter (80 nm). Although the exact mechanism of electrochemical etching on stainless steel is not fully understood, Kim et al. (2018) and Gao et al. (2017) observed that the WCAs decreased with the extended etching treatment duration possibly due to the increase in the local corrosion rate.

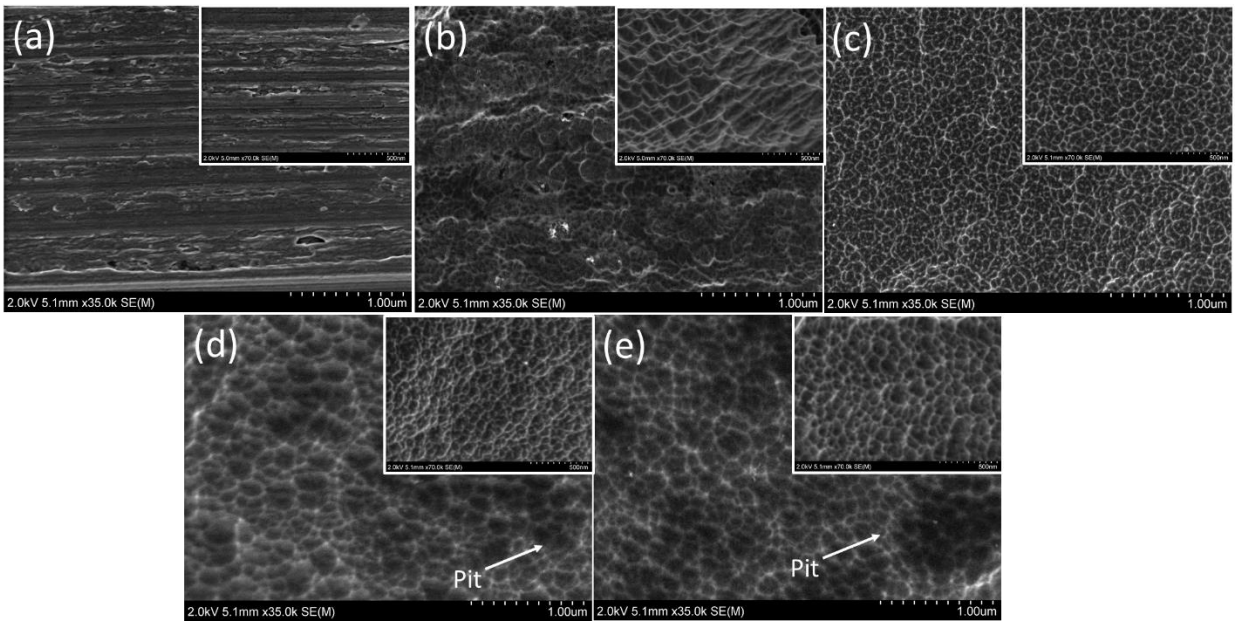

Figure 4.4. SEM images of 304 stainless steel surfaces: (a) bare, electrochemically etched at (b) 5 V 10 min, (c) 10 V 10 min (d) 15 V 10 min, (e) 15 V 15 min.

4.3.2. Effect of the superhydrophobic surface on the attachment of *L. monocytogenes*

Based on the previous findings (Figure 4.4), the anti-bacterial efficiency was assessed by monitoring the adhesion of *L. monocytogenes* on the bare and the fabricated superhydrophobic surfaces (Figure 4.5). The initial concentration of *L. monocytogenes* in the PBS solution was 9.2 log CFU/mL. The number of bacterial cells attached to the hydrophilic bare substrate was 6.1 log cm^{-2}. As expected, the number of bacterial cells colonized on the 10 V 5 min PTFE and 10 V 10 min PTFE SH surfaces were significantly reduced to 4.3, and 4.1 log CFU cm^{-2}, respectively. The SH surfaces are anti-bacterial due to their minimal solid-liquid contact at the surface and weak surface interactions with the bacterial cells. Therefore, it is more favorable for the bacteria to remain in the solution rather than adhering to the SH surface (Jeevahan et al., 2018). In addition,

air can be trapped between the rough surface and the bacterial suspension. Air pockets aid in repelling and reducing the contact area between the bacteria and the substrate (Ogihara, Xie & Saji, 2013; Sun et al., 2005). Tang et al. (2011) produced superhydrophobic surface by anodic oxidation with PTES on titanium surface and observed decrease in the adherence of *Staphylococcus aureus* (*S. aureus*). Freschauf et al. (2012) fabricated superhydrophobic polystyrene, polycarbonate, and polyethylene surfaces and observed 2% of the initial *Eschericia coli (E. coli*) cells adhered to these surfaces.

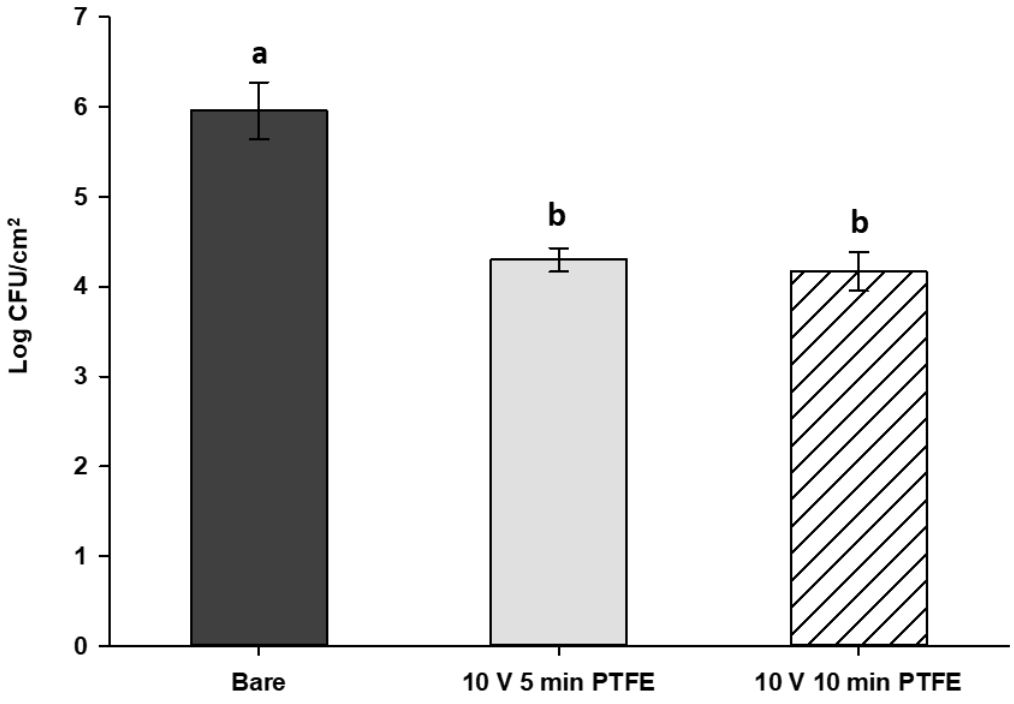

Figure 4.5. Populations of *L. monocytogenes* attached to surfaces of bare stainless steel, electrochemically etched stainless steel at 10 V 5 min and 10 min with PTFE coating.

4.3.3. Comparison of biofilm development on the native and superhydrophobic surface

The initial step in biofilm formation is a non-specific and reversible attachment of bacteria on surfaces. In order to create natural conditions, a CDC biofilm reactor was selected as a tool for growing a standard biofilm. The CDC biofilm reactor is reliable with the ability to mimic two nature-like environments-a renewable nutrient source and shear forces (Pérez-Conesa et al., 2011; Williams & Bloebaum, 2010). According to Figure 4.6, the native stainless steel surface attracted the bacteria the most. The level of *L. monocytogenes* cells enclosed in biofilms on the SH coupon (10 V 5 min PTFE) was significantly decreased by 98.4% compared to the native stainless steel surface. A possible reason could be due to the non-wetting behavior exhibited by the modified surfaces (WCA > 150°), which prevents the bacterial suspension to adsorb or spread over the surface. Additionally, the dynamic flow condition induced with the CDC biofilm reactor can sweep away the microbial cells and keep the underlying surface clean. This self-cleaning effect, attributing to the low adhesion force, is the key anti-bacterial properties of the SH surfaces. However, compared to the bacterial attachment results (Figure 4.5), a slightly decreased bacterial resistance behavior was observed in the flow environment. Although the details of the wetting transition are not fully understood yet, the superhydrophobic surface in the Cassie state could have transitioned to a metastable Cassie state due to the shear force applied by the CDC biofilm reactor. Sarkar & Kietzig (2015) have reported that the energy barrier between the wetting regime can be overcome by external factors such as gravity, drop deposition method, and pressure. Nevertheless, it appears that the SH coupons resisted bacterial adhesion entrapped in biofilms. Cheng et al. (2007) suggested that the low surface energy of the hydrophobic surface is likely to reduce bacterial adhesion by inducing reversible attachment or detachment of bacterial cells. Hizal et al. (2017) reported that the nanoengineered hydrophobic surfaces reduced the attachment of *S. aureus* and *E.*

coli K12 by more than 99.9% and 99.4%, respectively. Yoon et al. (2014) evaluated the adhesion of *E. coli* K12 on superhydrophobic nanocomposite surfaces and observed approximately 80% reduction in a fluid flow condition.

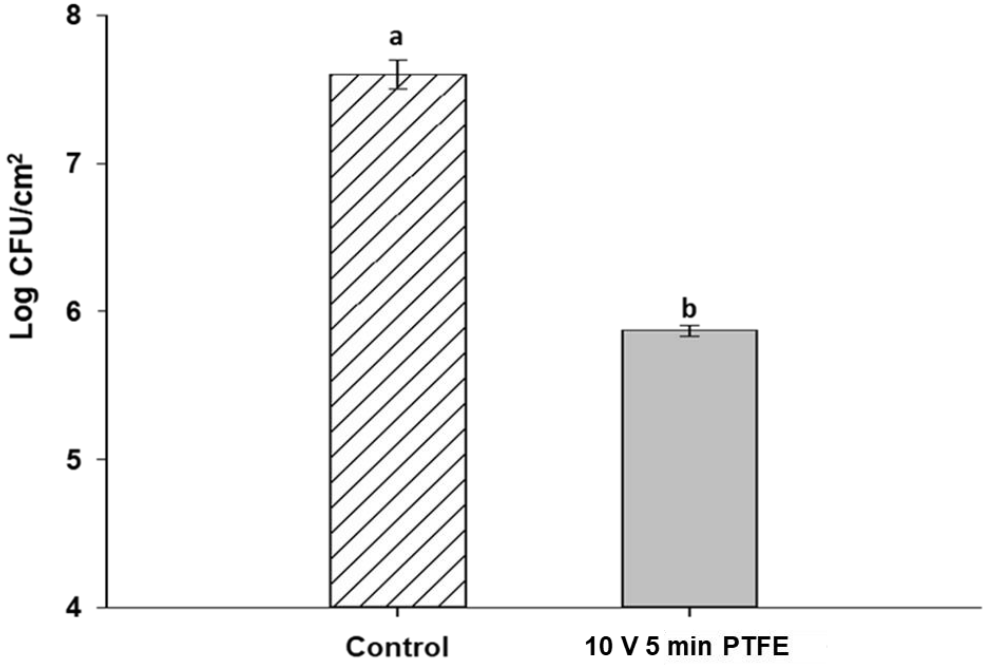

Figure 4.6. Viable counts of L. monocytogenes in biofilms formed on native and modified (10 V 5 min PTFE) coupons.

The SEM images of the *L. monocytogenes* biofilms on the control and SH surface are shown in Figure 4.7 ((a)-(d)). Compared to the developed superhydrophobic substrate, dense clusters of *L. monocytogenes* surrounded with matrix layers attaching to the substrate are evident on the native substrate. The images clearly illustrate that the SH surface resisted the bacterial attachment and biofilm formation to a greater extent as compared with the control surface.

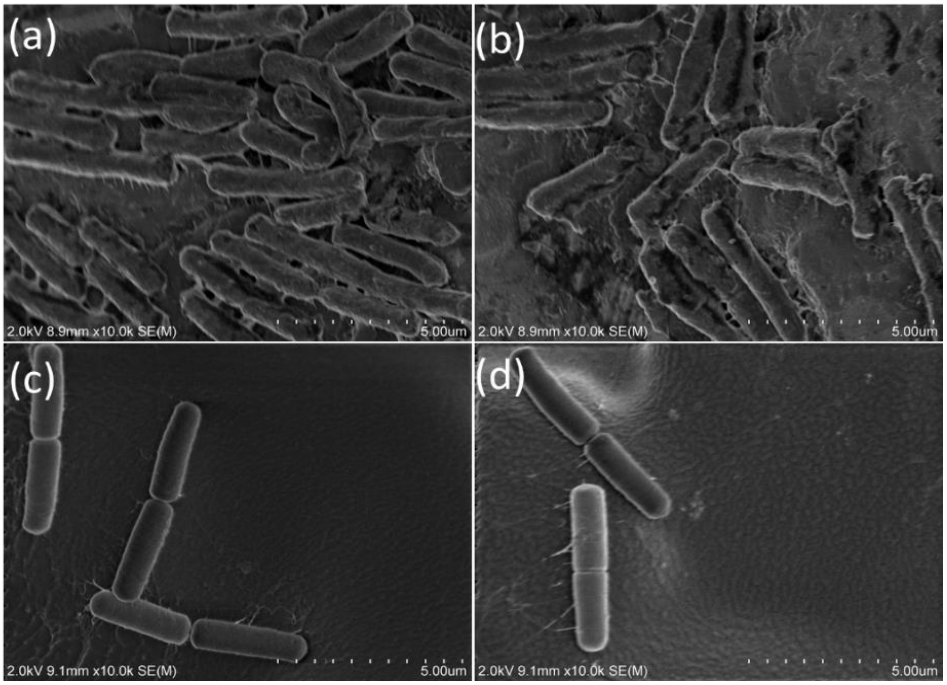

Figure 4.7. SEM images of *L. monocytogenes* biofilm on (a)-(b) native (c)-(d) modified (10 V 5 min PTFE) samples.

4.4. Conclusion

The present study successfully evaluated the applicability of electrochemical etching and PTFE coating in developing anti-bacterial nano-engineered surfaces. The stainless steel etched at 10 V for 5 min and 10 V for 10 min with PTFE deposition, being the most hydrophobic, demonstrated the highest increase in WCAs (154° ± 4°) with a pore diameter of 50 nm and decreased the adhesion of *L. monocytogenes* up to 99%. Corresponding to the bacterial adhesion assay result, the colonization of bacterial cells and the growth of biofilms were significantly less on the SH nanoporous surface compared to the bare surface. It was shown that the modification of surface topographical features at nanoscale was needed to achieve the desired bacterial and biofilm resisting properties. This surface modification technique has potential for anti-biofouling applications in the fruit and vegetable washer, thereby resulting in reduced cross-contamination and enhanced microbial quality of end products.

Chapter 5.

CONCLUSIONS AND FUTURE WORKS

This work has demonstrated the application of nanotechnology for the detection of bacteria and the fabrication of biofouling resistant surfaces. The incorporation of SWCNTs enhanced the sensing signal by 5-folds due to the amplification of the sensing platform surface area. The SWCNT-conjugated biosensor demonstrated a linear relationship ($R^2 = 0.982$) in response to 10^3 - 10^8 CFU/mL of *L. monocytogenes*. The response of the sensor against non-targets was investigated with *E. coli* O157:H7 and *S.* Typhimurium and the observed variations were miniscule. To fulfill the need of microbial analytical tools applicable in the field, the SWCNTs-based sensors were incorporated into a smartphone-controlled wireless platform. The sensing signal from the smartphone-controlled unit corresponded closely to the reference instrument in response to 10^3 – 10^5 CFU/mL of *L. monocytogenes* in both pure culture and a food sample.

Since the overall goal of this technology is to use as an on-site foodborne pathogen testing, the sensitivity of the sensor must be studied further. The current fabricated biosensor does not meet the industrial food safety requirement as the policy on *L. monocytogenes* in ready-to-eat foods is a zero (Archer, 2018; Shank et al., 1996). The sensitivity of the sensor could be enhanced by applying dielectrophoresis (DEP) force. DEP is the movement of particles in a solution that has been subjected to a non-uniform electric field (Pethig, 1996). DEP force can be used to electrically manipulate biological analytes within a fluid medium and increase the sensitivity. The sensing parameters such as the medium conductivity, applied voltage and frequency, and DEP exposure time in detecting bacterial pathogens in food samples should be further investigated. In addition, superparamagnetic particles such as magnetic beads and magnetic nanoparticles could be utilized.

The superparamagntic particles have been conjugated with various bioreceptors including antibodies and have shown to improve both the transduction signal and sensitivities due to their unique physical and chemical properties (Reverté, Prieto-Simón, & Campàs, 2016; Wang et al., 2017). When subjected to an external magnetic field, the superparamagnetic particles are magnetized and enables the magnetic manipulation and thus, detection of the bacterial cells without affecting the biological interactions. The performance of the immunosensor depends highly on the performance of the antibody. The antibody-antigen interaction is influenced by factors such as temperature, pH, ionic strength, and concentrations of antigen and antibody. Therefore, further studies should address the influence of the listed factors on the immobilization of antibodies as well as the affinity of the antibody.

The nanoengineered superhydrophobic surface was fabricated by the combination of electrochemical etching and PTFE film. The surfaces etched at 10 V for 5 min and 10 V for 10 min with PTFE deposition demonstrated the highest increase in the WCAs (154° ± 4°). The developed SH surface resisted the bacterial adhesion up to 99% and the population of bacteria enclosed in biofilms was decreased by 98.4%. The SEM images revealed that the fabricated SH surface enhanced the hydrophobicity by increasing the surface roughness with nanopores (50 nm) and the extent of biofilm formation was significantly less on the SH surface compared to the bare surface.

In the future, the surface roughness should be controlled by optimizing parameters such as the electrochemical etching voltage, time, and concentrations of acids to produce uniform pore sizes. In addition, different PTFE molding techniques such as dip coating can be investigated as well. Beckford & Zou (2014) coated PTFE films on stainless steel via insertion and withdrawl method at speed of 10 mm/min and achieved a total film thickness of approximately 580 nm. In

order to extend the anti-bacterial surface to industrial applications, thermodynamic, mechanical, and chemical robustness must be investigated. In the food industry, the SH surfaces can be exposed to dynamic situations and their stability under various conditions such as heat, humidity, corrosion, pH, and UV must be studied further.

REFERENCES

Ahmed, A., Rushworth, J. V., Hirst, N. A., & Millner, P. A. (2014). Biosensors for whole-cell bacterial detection. *Clinical Microbiology Reviews*, *27*(3), 631–646.

Akbas, M. Y. (2015). Bacterial biofilms and their new control strategies in food industry. *The Battle Against Microbial Pathogens: Basic Science, Technological Advances and Educational Programs, Badajoz: Formatex*, 383–394.

Allen, B. L., Kichambare, P. D., & Star, A. (2007). Carbon nanotube field-effect-transistor-based biosensors. *Advanced Materials*, *19*(11), 1439–1451.

Alocilja, E. C., & Radke, S. M. (2003). Market analysis of biosensors for food safety. *Biosensors and Bioelectronics*, *18*(5–6), 841–846.

Archer, D. L. (2018). The evolution of FDA's policy on Listeria monocytogenes in ready-to-eat foods in the United States. *Current Opinion in Food Science*, *20*, 64–68.

Arora, P., Sindhu, A., Dilbaghi, N., & Chaudhury, A. (2011). Biosensors as innovative tools for the detection of food borne pathogens. *Biosensors and Bioelectronics*, *28*(1), 1–12.

Bajpai, V. K., Kamle, M., Shukla, S., Mahato, D. K., Chandra, P., Hwang, S. K., … Han, Y. K. (2018). Prospects of using nanotechnology for food preservation, safety, and security. *Journal of Food and Drug Analysis*, *26*(4), 1201–1214.

Beckford, S., & Zou, M. (2014). Wear resistant PTFE thin film enabled by a polydopamine adhesive layer. *Applied Surface Science*, *292*, 350–356.

Berekaa, M. M (2015) Nanotechnology in food industry; advances in food processing packaging and food safety. *International Journal of Current Microbiology and Applied Sciences, 4*(5),

345-357

Bogomolova, A., Komarova, E., Reber, K., Gerasimov, T., Yavuz, O., Bhatt, S., & Aldissi, M. (2009). Challenges of electrochemical impedance spectroscopy in protein biosensing. *Analytical Chemistry*, *81*(10), 3944–3949.

Boinovich, L. B., Emelyanenko, A. M., Ivanov, V. K., & Pashinin, A. S. (2013). Durable icephobic coating for stainless steel. *ACS Applied Materials & Interfaces*, *5*(7), 2549–2554.

Bourigua, S., Hnaien, M., Bessueille, F., Lagarde, F., Dzyadevych, S., Maaref, A., … Renault, N. J. (2010). Impedimetric immunosensor based on SWCNT-COOH modified gold microelectrodes for label-free detection of deep venous thrombosis biomarker. *Biosensors and Bioelectronics*, *26*(4), 1278–1282.

Brooks, J. D., & Flint, S. H. (2008). Biofilms in the food industry: Problems and potential solutions. *International Journal of Food Science & Technology*, *43*(12), 2163–2176.

CDC. (2018). CDC and Food Safety. Retrieved from https://www.cdc.gov/foodsafety/cdc-and-food-safety.html

Chen, J., Zheng, X., Miao, F., Zhang, J., Cui, X., & Zheng, W. (2012). Engineering graphene/carbon nanotube hybrid for direct electron transfer of glucose oxidase and glucose biosensor. *Journal of Applied Electrochemistry*, *42*(10), 875–881.

Chen, Q., Wang, D., Cai, G., Xiong, Y., Li, Y., Wang, M., … Lin, J. (2016). Fast and sensitive detection of foodborne pathogen using electrochemical impedance analysis, urease catalysis and microfluidics. *Biosensors and Bioelectronics*, *86*, 770–776.

Chen, Y. Y., Duval, T., Hung, U. D., Yeh, J. W., & Shih, H. C. (2005). Microstructure and

electrochemical properties of high entropy alloys-a comparison with type-304 stainless steel. *Corrosion Science*, *47*(9), 2257–2279.

Cheng, G., Zhang, Z., Chen, S., Bryers, J. D., & Jiang, S. (2007). Inhibition of bacterial adhesion and biofilm formation on zwitterionic surfaces. *Biomaterials*, *28*(29), 4192–4199.

Chmielewski, R. A. N., & Frank, J. F. (2003). Biofilm formation and control in food processing facilities. *Comprehensive Reviews in Food Science and Food Safety*, *2*(1), 22–32.

Chowdhury, A. D., De, A., Chaudhuri, C. R., Bandyopadhyay, K., & Sen, P. (2012). Label free polyaniline based impedimetric biosensor for detection of E. coli O157: H7 Bacteria. *Sensors and Actuators B: Chemical*, *171*, 916–923.

Chunglok, W., Wuragil, D. K., Oaew, S., Somasundrum, M., & Surareungchai, W. (2011). Immunoassay based on carbon nanotubes-enhanced ELISA for Salmonella enterica serovar Typhimurium. *Biosensors and Bioelectronics*, *26*(8), 3584–3589.

Conroy, P. J., Hearty, S., Leonard, P., & O'Kennedy, R. J. (2009). Antibody production, design and use for biosensor-based applications. *Seminars in Cell & Developmental Biology*, *20*(1), 10–26.

Costa, C. A., Luciano, M. A., & Pasa, A. M. (2013). Guiding criteria for hygienic design of food industry equipment. *Journal of Food Process Engineering*, *36*(6), 753–762.

Crick, C. R., Ismail, S., Pratten, J., & Parkin, I. P. (2011). An investigation into bacterial attachment to an elastomeric superhydrophobic surface prepared via aerosol assisted deposition. *Thin Solid Films*, *519*(11), 3722–3727.

Cvetkovski, S. (2012). Stainless steel in contact with food and bevarage. *Metallurgical and*

Materials Engineering, *18*(4), 283–294.

Darmanin, T., de Givenchy, E. T., Amigoni, S., & Guittard, F. (2013). Superhydrophobic surfaces by electrochemical processes. *Advanced Materials*, *25*(10), 1378–1394.

Darst, S. A., Ahlers, M., Meller, P. H., Kubalek, E. W., Blankenburg, R., Ribi, H. O., … Kornberg, R. D. (1991). Two-dimensional crystals of streptavidin on biotinylated lipid layers and their interactions with biotinylated macromolecules. *Biophysical Journal*, *59*(2), 387–396.

de Boer, E., & Beumer, R. R. (1999). Methodology for detection and typing of foodborne microorganisms. *International Journal of Food Microbiology*, *50*(1–2), 119–130.

Dhanumalayan, E., & Joshi, G. M. (2018). Performance properties and applications of polytetrafluoroethylene (PTFE)-a review. *Advanced Composites and Hybrid Materials*, *1*(2), 247–268.

Donlan, R. M. (2002). Biofilms: microbial life on surfaces. *Emerging Infectious Diseases*, *8*(9), 881.

Durrani, S. A., & Bull, R. K. (2013). *Solid state nuclear track detection: principles, methods and applications*. Elsevier.

Dweik, M., Stringer, R. C., Dastider, S. G., Wu, Y., Almasri, M., & Barizuddin, S. (2012). Specific and targeted detection of viable Escherichia coli O157: H7 using a sensitive and reusable impedance biosensor with dose and time response studies. *Talanta*, *94*, 84–89.

Ebnesajjad, S. (2016). *Expanded PTFE applications handbook: technology, manufacturing and applications*. William Andrew.

Feng, M., Yong, Q., Wang, W., Kuang, H., Wang, L., & Xu, C. (2013). Development of a

monoclonal antibody-based ELISA to detect Escherichia coli O157: H7. *Food and Agricultural Immunology*, *24*(4), 481–487.

Ferrier, D. C., Shaver, M. P., & Hands, P. J. W. (2015). Micro-and nano-structure based oligonucleotide sensors. *Biosensors and Bioelectronics*, *68*, 798–810.

Ferreira, F. V., Franceschi, W., Menezes, B. R., Biagioni, A. F., Coutinho, A. R., & Cividanes, L. S. (2019). Synthesis, Characterization, and Applications of Carbon Nanotubes. In Carbon-Based Nanofillers and Their Rubber Nanocomposites (pp. 1-45). Elsevier.

Frank, J. F., & Koffi, R. A. (1990). Surface-adherent growth of Listeria monocytogenes is associated with increased resistance to surfactant sanitizers and heat. *Journal of Food Protection*, *53*(7), 550–554.

Freschauf, L. R., McLane, J., Sharma, H., & Khine, M. (2012). Shrink-induced superhydrophobic and antibacterial surfaces in consumer plastics. *PLoS One*, *7*(8), e40987.

Garrett, T. R., Bhakoo, M., & Zhang, Z. (2008). Bacterial adhesion and biofilms on surfaces. *Progress in Natural Science*, *18*(9), 1049–1056.

Gaudin, V. (2017). Advances in biosensor development for the screening of antibiotic residues in food products of animal origin-A comprehensive review. *Biosensors and Bioelectronics*, *90*, 363–377.

Gibson, H., Taylor, J. H., Hall, K. E., & Holah, J. T. (1999). Effectiveness of cleaning techniques used in the food industry in terms of the removal of bacterial biofilms. *Journal of Applied Microbiology*, *87*(1), 41–48.

Gillett, A., Waugh, D., Lawrence, J., Swainson, M., & Dixon, R. (2016). Laser surface

modification for the prevention of biofouling by infection causing Escherichia Coli. *Journal of Laser Applications*, *28*(2), 22503.

Gu, H., & Ren, D. (2014). Materials and surface engineering to control bacterial adhesion and biofilm formation: A review of recent advances. *Frontiers of Chemical Science and Engineering*, *8*(1), 20–33.

Heller, I., Janssens, A. M., Männik, J., Minot, E. D., Lemay, S. G., & Dekker, C. (2008). Identifying the mechanism of biosensing with carbon nanotube transistors. *Nano Letters*, *8*(2), 591–595.

Herald, P. J., & Zottola, E. A. (1988). Scanning electron microscopic examination of Yersinia enterocolitica attached to stainless steel at selected temperatures and pH values. *Journal of Food Protection*, *51*(6), 445–448.

Hizal, F., Rungraeng, N., Lee, J., Jun, S., Busscher, H. J., Van Der Mei, H. C., & Choi, C. H. (2017). Nanoengineered superhydrophobic surfaces of aluminum with extremely low bacterial adhesivity. *ACS Applied Materials & Interfaces*, *9*(13), 12118–12129.

Hoffman, S., Maculloch, B., & Batz, M. (2015). Economic burden of major foodborne illnesses acquired in the United States. EIB-140. *US Department of Agriculture, Economic Research Service.*

Holzinger, M., Le Goff, A., & Cosnier, S. (2014). Nanomaterials for biosensing applications: a review. *Frontiers in Chemistry*, *2*, 63.

Hood, S. K., & Zottola, E. A. (1995). Biofilms in food processing. *Food Control*, *6*(1), 9–18.

Hsu, C. F., Tsai, T. Y., & Pan, T. M. (2005). Use of the duplex TaqMan PCR system for detection

of Shiga-like toxin-producing Escherichia coli O157. *Journal of Clinical Microbiology*, *43*(6), 2668–2673.

Huang, J., Yang, G., Meng, W., Wu, L., Zhu, A., & Jiao, X. (2010). An electrochemical impedimetric immunosensor for label-free detection of Campylobacter jejuni in diarrhea patients' stool based on O-carboxymethylchitosan surface modified Fe_3O_4 nanoparticles. *Biosensors and Bioelectronics*, *25*(5), 1204–1211.

Jadhav, S., Bhave, M., & Palombo, E. A. (2012). Methods used for the detection and subtyping of Listeria monocytogenes. *Journal of Microbiological Methods*, *88*(3), 327–341.

Jain, S., Singh, S. R., Horn, D. W., Davis, V. A., Ram, M. J., & Pillai, S. R. (2012). Development of an antibody functionalized carbon nanotube biosensor for foodborne bacterial pathogens. *J Biosens Bioelectron*, *11*, 2.

Jang, Y., Choi, W. T., Johnson, C. T., García, A. J., Singh, P. M., Breedveld, V., … Champion, J. A. (2017). Inhibition of bacterial adhesion on nanotextured stainless steel 316L by electrochemical etching. *ACS Biomaterials Science & Engineering*, *4*(1), 90–97.

Jenkins, D. M., Lee, B. E., Jun, S., Reyes-De-Corcuera, J., & McLamore, E. S. (2019). ABE-stat, a Fully Open-Source and Versatile Wireless Potentiostat Project Including Electrochemical Impedance Spectroscopy. *Journal of The Electrochemical Society*, *166*(9), B3056-B3065.

Jeżowski, P., Nowicki, M., Grzeszkowiak, M., Czajka, R., & Beguin, F. (2015). Chemical etching of stainless steel 301 for improving performance of electrochemical capacitors in aqueous electrolyte. *Journal of Power Sources*, *279*, 555–562.

Jimenez-Ruiz, A., Perez-Tejeda, P., Grueso, E., Castillo, P. M., & Prado-Gotor, R. (2015).

Nonfunctionalized gold nanoparticles: synthetic routes and synthesis condition dependence. *Chemistry-A European Journal*, *21*(27), 9596–9609.

Juneja, S., & Bhattacharya, J. (2019). Coffee ring effect assisted improved S. aureus screening on a physically restrained gold nanoflower enriched SERS substrate. *Colloids and Surfaces B: Biointerfaces*, *182*, 110349.

Kam, N. W. S., & Dai, H. (2005). Carbon nanotubes as intracellular protein transporters: generality and biological functionality. *Journal of the American Chemical Society*, *127*(16), 6021–6026.

Kamegawa, T., Shimizu, Y., & Yamashita, H. (2012). Superhydrophobic surfaces with photocatalytic self-cleaning properties by nanocomposite coating of TiO_2 and polytetrafluoroethylene. *Advanced Materials*, *24*(27), 3697–3700.

Kang, Y., & Taton, T. A. (2003). Micelle-encapsulated carbon nanotubes: a route to nanotube composites. *Journal of the American Chemical Society*, *125*(19), 5650–5651.

Keskinen, L. A., Burke, A., & Annous, B. A. (2009). Efficacy of chlorine, acidic electrolyzed water and aqueous chlorine dioxide solutions to decontaminate Escherichia coli O157: H7 from lettuce leaves. *International Journal of Food Microbiology*, *132*(2–3), 134–140.

Kim, H. J., Lee, H. J., Lee, K. H., & Cho, J. C. (2012). Simultaneous detection of Pathogenic Vibrio species using multiplex real-time PCR. *Food Control*, *23*(2), 491–498.

Kruse, H. (1999). Globalization of the food supply-food safety implications: special regional requirements: future concerns. *Food Control*, *10*(4–5), 315–320.

Kumar, C. G., & Anand, S. K. (1998). Significance of microbial biofilms in food industry: A review. *International Journal of Food Microbiology*, *42*(1–2), 9–27.

Kutz, M. (2018). *Handbook of environmental degradation of materials*. William Andrew.

Kuusela, P., Moran, A. P., Vartio, T., & Kosunen, T. U. (1989). Interaction of Campylobacter jejuni with extracellular matrix components. *Biochimica et Biophysica Acta (BBA)-General Subjects*, *993*(2–3), 297–300.

Lau, K. K. S., Bico, J., Teo, K. B. K., Chhowalla, M., Amaratunga, G. A. J., Milne, W. I., … Gleason, K. K. (2003). Superhydrophobic carbon nanotube forests. *Nano Letters*, *3*(12), 1701–1705.

Lee, C. K., & Shih, H. C. (1996). Effect of halide ions on electrochemical behavior and stress corrosion cracking of 67/33 α-Brass in Aqueous environments. *Corrosion*, *52*(9), 690–696.

Lee, K., Lee, J. W., Dong, K. Y., & Ju, B. K. (2008). Gas sensing properties of single-wall carbon nanotubes dispersed with dimethylformamide. *Sensors and Actuators B: Chemical*, *135*(1), 214–218.

Lee, S. H., & Frank, J. F. (1991). Inactivation of surface-adherent Listeria monocytogenes hypochlorite and heat. *Journal of Food Protection*, *54*(1), 4–6.

Lelieveld, H. L. M., Mostert, M. A., & Curiel, G. J. (2014). Hygienic design of food processing equipment. In *Hygiene in Food Processing*. Elsevier.

Leonard, P., Hearty, S., Brennan, J., Dunne, L., Quinn, J., Chakraborty, T., & O'Kennedy, R. (2003). Advances in biosensors for detection of pathogens in food and water. *Enzyme and Microbial Technology*, *32*(1), 3–13.

Lin, Y., Taylor, S., Li, H., Fernando, K. A. S., Qu, L., Wang, W., … Sun, Y. P. (2004). Advances toward bioapplications of carbon nanotubes. *Journal of Materials Chemistry*, *14*(4), 527–541.

Lisdat, F., & Schäfer, D. (2008). The use of electrochemical impedance spectroscopy for biosensing. *Analytical and Bioanalytical Chemistry*, *391*(5), 1555.

Liu, Y., Bai, Y., Jin, J., Tian, L., Han, Z., & Ren, L. (2015). Facile fabrication of biomimetic superhydrophobic surface with anti-frosting on stainless steel substrate. *Applied Surface Science*, *355*, 1238–1244.

Lu, L., Chee, G., Yamada, K., & Jun, S. (2013). Electrochemical impedance spectroscopic technique with a functionalized microwire sensor for rapid detection of foodbornepathogens. *Biosensors and Bioelectronics*, *42*, 492–495.

Majumdar, T., Chakraborty, R., & Raychaudhuri, U. (2013). Development of PEI-GA modified antibody based sensor for the detection of S. aureus in food samples. *Food Bioscience*, *4*, 38–45.

Mandal, P. K., Biswas, A. K., Choi, K., & Pal, U. K. (2011). Methods for rapid detection of foodborne pathogens: An overview. *American Journal of Food Technology*, *6*(2), 87–102.

Mao, Y., Huang, X., Xiong, S., Xu, H., Aguilar, Z. P., & Xiong, Y. (2016). Large-volume immunomagnetic separation combined with multiplex PCR assay for simultaneous detection of Listeria monocytogenes and Listeria ivanovii in lettuce. *Food Control*, *59*, 601–608.

Marmur, A. (2003). Wetting on hydrophobic rough surfaces: to be heterogeneous or not to be? *Langmuir*, *19*(20), 8343–8348.

Mello, L. D., & Kubota, L. T. (2002). Review of the use of biosensors as analytical tools in the food and drink industries. *Food Chemistry*, *77*(2), 237–256.

Meyer, B. (2003). Approaches to prevention, removal and killing of biofilms. *International*

Biodeterioration & Biodegradation, *51*(4), 249–253.

Mittelman, M. W. (1998). Structure and functional characteristics of bacterial biofilms in fluid processing operations. *Journal of Dairy Science*, *81*(10), 2760–2764.

Mohamed, A. M. A., Abdullah, A. M., & Younan, N. A. (2015). Corrosion behavior of superhydrophobic surfaces: A review. *Arabian Journal of Chemistry*, *8*(6), 749–765.

Møretrø, T., & Langsrud, S. (2004). Listeria monocytogenes: biofilm formation and persistence in food-processing environments. *Biofilms*, *1*(2), 107–121.

Nam, H. M., Srinivasan, V., Gillespie, B. E., Murinda, S. E., & Oliver, S. P. (2005). Application of SYBR green real-time PCR assay for specific detection of Salmonella spp. in dairy farm environmental samples. *International Journal of Food Microbiology*, *102*(2), 161–171.

Norwood, D. E., & Gilmour, A. (2000). The growth and resistance to sodium hypochlorite of Listeria monocytogenes in a steady-state multispecies biofilm. *Journal of Applied Microbiology*, *88*(3), 512–520.

Nosonovsky, M., & Bhushan, B. (2008). Roughness-induced superhydrophobicity: A way to design non-adhesive surfaces. *Journal of Physics: Condensed Matter*, *20*(22), 225009.

Nyachuba, D. G. (2010). Foodborne illness: is it on the rise? *Nutrition Reviews*, *68*(5), 257–269.

Odom, T. W., Huang, J. L., Kim, P., & Lieber, C. M. (2000). *Structure and electronic properties of carbon nanotubes*. ACS Publications.

Ogihara, H., Xie, J., & Saji, T. (2013). Factors determining wettability of superhydrophobic paper prepared by spraying nanoparticle suspensions. *Colloids and Surfaces A: Physicochemical and Engineering Aspects*, *434*, 35–41.

Öner, D., & McCarthy, T. J. (2000). Ultrahydrophobic surfaces. Effects of topography length scales on wettability. *Langmuir*, *16*(20), 7777–7782.

Patankar, N. A. (2004). Transition between superhydrophobic states on rough surfaces. *Langmuir*, *20*(17), 7097-7102.

Pathakoti, K., Manubolu, M., & Hwang, H. M. (2017). Nanostructures: Current uses and future applications in food science. *Journal of Food and Drug Analysis*, *25*(2), 245–253.

Pérez-Conesa, D., Cao, J., Chen, L., McLandsborough, L., & Weiss, J. (2011). Inactivation of Listeria monocytogenes and Escherichia coli O157: H7 biofilms by micelle-encapsulated eugenol and carvacrol. *Journal of Food Protection*, *74*(1), 55–62.

Pernites, R. B., Santos, C. M., Maldonado, M., Ponnapati, R. R., Rodrigues, D. F., & Advincula, R. C. (2011). Tunable protein and bacterial cell adsorption on colloidally templated superhydrophobic polythiophene films. *Chemistry of Materials*, *24*(5), 870–880.

Pethig, R. (1996). Dielectrophoresis: using inhomogeneous AC electrical fields to separate and manipulate cells. *Critical Reviews in Biotechnology*, *16*(4), 331–348.

Privett, B. J., Youn, J., Hong, S. A., Lee, J., Han, J., Shin, J. H., & Schoenfisch, M. H. (2011). Antibacterial fluorinated silica colloid superhydrophobic surfaces. *Langmuir*, *27*(15), 9597–9601.

Putzbach, W., & Ronkainen, N. (2013). Immobilization techniques in the fabrication of nanomaterial-based electrochemical biosensors: A review. *Sensors*, *13*(4), 4811–4840.

Ren, W., Ballou, D. R., FitzGerald, R., & Irudayaraj, J. (2019). Plasmonic enhancement in lateral flow sensors for improved sensing of E. coli O157: H7. *Biosensors and Bioelectronics*, *126*,

324–331.

Reverté, L., Prieto-Simón, B., & Campàs, M. (2016). New advances in electrochemical biosensors for the detection of toxins: Nanomaterials, magnetic beads and microfluidics systems. A review. *Analytica chimica acta, 908*, 8-21.

Sandu, C., & Singh, R. K. (1991). Energy increase in operation and cleaning due to heat-exchanger fouling in milk pasteurization. *Food Technology (USA)*.

Sarkar, A., & Kietzig, A. M. (2015). Design of a robust superhydrophobic surface: thermodynamic and kinetic analysis. *Soft Matter*, *11*(10), 1998-2007.

Sauer, K., Rickard, A. H., & Davies, D. G. (2007). Biofilms and biocomplexity. *Microbe-American Society for Microbiology, 2*(7), 347.

Scallan, E., Hoekstra, R. M., Angulo, F. J., Tauxe, R. V, Widdowson, M. A., Roy, S. L., … Griffin, P. M. (2011). Foodborne illness acquired in the United States-major pathogens. *Emerging Infectious Diseases*, *17*(1), 7.

Scher, K., Romling, U., & Yaron, S. (2005). Effect of heat, acidification, and chlorination on Salmonella enterica serovar Typhimurium cells in a biofilm formed at the air-liquid interface. *Applied and Enviornmental Microbiology*, *71*(3), 1163–1168.

Shank, F. R., Elliot, E. L., Wachsmuth, I. K., & Losikoff, M. E. (1996). US position on Listeria monocytogenes in foods. *Food Control, 7*(4–5), 229–234.

Sharma, H., & Mutharasan, R. (2013). Review of biosensors for foodborne pathogens and toxins. *Sensors and Actuators B: Chemical*, *183*, 535–549.

Shi, J., Chan, C., Pang, Y., Ye, W., Tian, F., Lyu, J., … Yang, M. (2015). A fluorescence resonance

energy transfer (FRET) biosensor based on graphene quantum dots (GQDs) and gold nanoparticles (AuNPs) for the detection of mecA gene sequence of Staphylococcus aureus. *Biosensors and Bioelectronics*, *67*, 595–600.

Si, S. H., Li, X., Fung, Y. S., & Zhu, D. R. (2001). Rapid detection of Salmonella enteritidis by piezoelectric immunosensor. *Microchemical Journal*, *68*(1), 21–27.

Silk, B. J., McCoy, M. H., Iwamoto, M., & Griffin, P. M. (2014). Foodborne listeriosis acquired in hospitals. *Clinical Infectious Diseases*, *59*(4), 532–540.

Simões, M., Simões, L. C., & Vieira, M. J. (2010). A review of current and emergent biofilm control strategies. *LWT-Food Science and Technology*, *43*(4), 573–583.

Singh, A., Poshtiban, S., & Evoy, S. (2013). Recent advances in bacteriophage based biosensors for food-borne pathogen detection. *Sensors*, *13*(2), 1763–1786.

Sireesha, M., Jagadeesh Babu, V., Kranthi Kiran, A. S., & Ramakrishna, S. (2018). A review on carbon nanotubes in biosensor devices and their applications in medicine. *Nanocomposites*, *4*(2), 36–57.

Somers, E. B., Schoeni, J. L., & Wong, A. C. L. (1994). Effect of trisodium phosphate on biofilm and planktonic cells of Campylobacter jejuni, Escherichia coli O157: H7, Listeria monocytogenes and Salmonella typhimurium. *International Journal of Food Microbiology*, *22*(4), 269–276.

Sozer, N., & Kokini, J. L. (2009). Nanotechnology and its applications in the food sector. *Trends in Biotechnology*, *27*(2), 82–89.

Srey, S., Jahid, I. K., & Ha, S. D. (2013). Biofilm formation in food industries: A food safety

concern. *Food Control*, *31*(2), 572–585.

Sun, T., Feng, L., Gao, X., & Jiang, L. (2005). Bioinspired surfaces with special wettability. *Accounts of Chemical Research*, *38*(8), 644–652.

Sun, T., Tan, H., Han, D., Fu, Q., & Jiang, L. (2005). No platelet can adhere-largely improved blood compatibility on nanostructured superhydrophobic surfaces. *Small*, *1*(10), 959–963.

Swaminathan, B., & Gerner-Smidt, P. (2007). The epidemiology of human listeriosis. *Microbes and Infection*, *9*(10), 1236–1243.

Tang, P., Zhang, W., Wang, Y., Zhang, B., Wang, H., Lin, C., & Zhang, L. (2011). Effect of superhydrophobic surface of titanium on staphylococcus aureus adhesion. *Journal of Nanomaterials*, *2011*, 2.

Taylor, A. D., Ladd, J., Yu, Q., Chen, S., Homola, J., & Jiang, S. (2006). Quantitative and simultaneous detection of four foodborne bacterial pathogens with a multi-channel SPR sensor. *Biosensors and Bioelectronics*, *22*(5), 752–758.

Timmons, C., Dobhal, S., Fletcher, J., & Ma, L. M. (2013). Primers with 5′ flaps improve the efficiency and sensitivity of multiplex PCR assays for the detection of Salmonella and Escherichia coli O157: H7. *Journal of Food Protection*, *76*(4), 668–673.

Van Houdt, R., & Michiels, C. W. (2010). Biofilm formation and the food industry, a focus on the bacterial outer surface. *Journal of Applied Microbiology*, *109*(4), 1117–1131.

Vashist, S. K., Schneider, E. M., Zengerle, R., von Stetten, F., & Luong, J. H. T. (2015). Graphene-based rapid and highly-sensitive immunoassay for C-reactive protein using a smartphone-based colorimetric reader. *Biosensors and Bioelectronics*, *66*, 169–176.

Velusamy, V., Arshak, K., Korostynska, O., Oliwa, K., & Adley, C. (2010). An overview of foodborne pathogen detection: In the perspective of biosensors. *Biotechnology Advances, 28*(2), 232–254.

Wang, B., Wang, Q., Cai, Z., & Ma, M. (2015). Simultaneous, rapid and sensitive detection of three food-borne pathogenic bacteria using multicolor quantum dot probes based on multiplex fluoroimmunoassay in food samples. *LWT-Food Science and Technology, 61*(2), 368–376.

Wang, L. J., Chang, Y. C., Sun, R., & Li, L. (2017). A multichannel smartphone optical biosensor for high-throughput point-of-care diagnostics. *Biosensors and Bioelectronics, 87*, 686–692.

Wang, R., Ruan, C., Kanayeva, D., Lassiter, K., & Li, Y. (2008). TiO_2 nanowire bundle microelectrode based impedance immunosensor for rapid and sensitive detection of Listeria monocytogenes. *Nano Letters, 8*(9), 2625–2631.

Wang, Y., Ye, Z., Si, C., & Ying, Y. (2011). Subtractive inhibition assay for the detection of E. coli O157: H7 using surface plasmon resonance. *Sensors, 11*(3), 2728–2739.

Wang, Y., Ye, Z., & Ying, Y. (2012). New trends in impedimetric biosensors for the detection of foodborne pathogenic bacteria. *Sensors, 12*(3), 3449–3471.

Wang, Z., Su, Y., Li, Q., Liu, Y., She, Z., Chen, F., … Zhang, P. (2015). Researching a highly anti-corrosion superhydrophobic film fabricated on AZ91D magnesium alloy and its anti-bacteria adhesion effect. *Materials Characterization, 99*, 200–209.

Wang, Zhouli, Yue, T., Yuan, Y., Cai, R., Niu, C., & Guo, C. (2013). Development and evaluation of an immunomagnetic separation-ELISA for the detection of Alicyclobacillus spp. in apple juice. *International Journal of Food Microbiology, 166*(1), 28–33.

Wang, T., Zhou, Y., Lei, C., Luo, J., Xie, S., & Pu, H. (2017). Magnetic impedance biosensor: A review. *Biosensors and Bioelectronics, 90*, 418-435.

Williams, D. L., & Bloebaum, R. D. (2010). Observing the biofilm matrix of Staphylococcus epidermidis ATCC 35984 grown using the CDC biofilm reactor. *Microscopy and Microanalysis*, *16*(2), 143–152.

Wong, Y. Y., Ng, S. P., Ng, M. H., Si, S. H., Yao, S. Z., & Fung, Y. S. (2002). Immunosensor for the differentiation and detection of Salmonella species based on a quartz crystal microbalance. *Biosensors and Bioelectronics*, *17*(8), 676–684.

Xu, X., Yuan, Y., Hu, G., Wang, X., Qi, P., Wang, Z., … Yang, H. (2017). Exploiting pH-regulated dimer-tetramer transformation of concanavalin a to develop colorimetric biosensing of bacteria. *Scientific Reports*, *7*(1), 1452.

Yamada, K., Kim, C. T., Kim, J. H., Chung, J. H., Lee, H. G., & Jun, S. (2014). Single walled carbon nanotube-based junction biosensor for detection of Escherichia coli. *PloS One*, *9*(9), e105767.

Yang, Y. F., Li, Y., Li, Q. L., Wan, L. S., & Xu, Z. K. (2010). Surface hydrophilization of microporous polypropylene membrane by grafting zwitterionic polymer for anti-biofouling. *Journal of Membrane Science*, *362*(1–2), 255–264.

Yin, B., Wang, Y., Dong, M., Wu, J., Ran, B., Xie, M., … Chen, Y. (2016). One-step multiplexed detection of foodborne pathogens: Combining a quantum dot-mediated reverse assaying strategy and magnetic separation. *Biosensors and Bioelectronics*, *86*, 996–1002.

Yoo, M. S., Shin, M., Kim, Y., Jang, M., Choi, Y. E., Park, S. J., … Park, C. (2017). Development

of electrochemical biosensor for detection of pathogenic microorganism in Asian dust events. *Chemosphere*, *175*, 269–274.

Yoo, S. M., Baek, Y. K., Shin, S. H. R., Kim, J. H., Jung, H. T., Choi, Y. K., & Lee, S. Y. (2016). Single walled carbon nanotube-based electrical biosensor for the label-free detection of pathogenic bacteria. *Journal of Nanoscience and Nanotechnology*, *16*(6), 6520–6525.

Yoon, S. H., Rungraeng, N., Song, W., & Jun, S. (2014). Superhydrophobic and superhydrophilic nanocomposite coatings for preventing Escherichia coli K-12 adhesion on food contact surface. *Journal of Food Engineering*, *131*, 135–141.

Yun, Y., Bange, A., Heineman, W. R., Halsall, H. B., Shanov, V. N., Dong, Z., … Wong, D. K. (2007). A nanotube array immunosensor for direct electrochemical detection of antigen-antibody binding. *Sensors and Actuators B: Chemical*, *123*(1), 177–182.

Zangheri, M., Cevenini, L., Anfossi, L., Baggiani, C., Simoni, P., Di Nardo, F., & Roda, A. (2015). A simple and compact smartphone accessory for quantitative chemiluminescence-based lateral flow immunoassay for salivary cortisol detection. *Biosensors and Bioelectronics*, *64*, 63–68.

Zhang, D., Jiang, J., Chen, J., Zhang, Q., Lu, Y., Yao, Y., … Liu, Q. (2015). Smartphone-based portable biosensing system using impedance measurement with printed electrodes for 2, 4, 6-trinitrotoluene (TNT) detection. *Biosensors and Bioelectronics*, *70*, 81–88.

Zhang, D., & Liu, Q. (2016). Biosensors and bioelectronics on smartphone for portable biochemical detection. *Biosensors and Bioelectronics*, *75*, 273–284.

Zhang, G. (2013). Foodborne pathogenic bacteria detection: an evaluation of current and

developing methods. *The Meducator*, *1*(24).

Zhang, X., Wang, L., & Levänen, E. (2013). Superhydrophobic surfaces for the reduction of bacterial adhesion. *Rsc Advances*, *3*(30), 12003–12020.

Zhao, X., Lin, C. W., Wang, J., & Oh, D. H. (2014). Advances in rapid detection methods for foodborne pathogens. *Journal of Microbiology and Biotechnology*, *24*(3), 297–312.

Zheng, L., Cai, G., Wang, S., Liao, M., Li, Y., & Lin, J. (2019). A microfluidic colorimetric biosensor for rapid detection of Escherichia coli O157: H7 using gold nanoparticle aggregation and smart phone imaging. *Biosensors and Bioelectronics*, *124*, 143–149.

Zhou, H., Yang, D., Ivleva, N. P., Mircescu, N. E., Niessner, R., & Haisch, C. (2014). SERS detection of bacteria in water by in situ coating with Ag nanoparticles. *Analytical Chemistry*, *86*(3), 1525–1533.

Zhou, R., Wang, P., & Chang, H. C. (2006). Bacteria capture, concentration and detection by alternating current dielectrophoresis and self-assembly of dispersed single-wall carbon nanotubes. *Electrophoresis*, *27*(7), 1376–1385.

Zhu, Q., Gooneratne, R., & Hussain, M. (2017). Listeria monocytogenes in fresh produce: outbreaks, prevalence and contamination levels. *Foods*, *6*(3), 21.

Zhuang, D., & Edgar, J. H. (2005). Wet etching of GaN, AlN, and SiC: A review. *Materials Science and Engineering: R: Reports*, *48*(1), 1–46.